University of the Pacific Theses and Dissertations

University Libraries

2023

Enhancing the half-life of Interleukin 2 by conjugation to the Transthyretin Ligand, TLHE And Enhancing the efficacy of peptides that inhibit COVID 19 viral entry

Arjun D. Patel
University of the Pacific

Follow this and additional works at: https://scholarlycommons.pacific.edu/uop_etds

Part of the Medicine and Health Sciences Commons

Recommended Citation

Enhancing the half-life of Interleukin 2 by conjugation to the Transthyretin Ligand, TLHE
And
Enhancing the efficacy of peptides that inhibit COVID 19 viral entry

By

Arjun D Patel

A Dissertation Submitted

In Partial Fulfillment of the

Requirements for the Degree of

DOCTOR OF PHILOSOPHY

Thomas J. Long School of Pharmacy
Pharmaceutical and Chemical Sciences

University of the Pacific
Stockton, California

2023

Enhancing the half-life of Interleukin 2 by conjugation to the Transthyretin Ligand, TLHE
And
Enhancing the efficacy of peptides that inhibit COVID 19 viral entry

By

Arjun D Patel

APPROVED BY:

Dissertation Advisor: Mamoun M. Alhamadsheh, Ph.D..

Committee Member: Miki S. Park, Ph.D

Committee Member: William K. Chan, Pharm.D., Ph.D.

Committee Member: David Thomas, Ph.D.

Committee Member: Qinliang Zhao, Ph.D.

Department Chair: William K. Chan, Pharm.D., Ph.D.

Enhancing the half-life of Interleukin 2 by conjugation to the Transthyretin Ligand, TLHE
And
Enhancing the efficacy of peptides that inhibit COVID 19 viral entry

Copyright 2023

By

Arjun D Patel

Dedication

To my loving, and ever generous parents, Devyani and Dilip Patel. I do not know what I did to deserve such angels in the form of a mother and father, but I will be forever indebted to them for their infinite love. I would also like to dedicate my work to Shankar Dutt Sharma. मनश्चैन लग्नम, गुरोरंघ्रि पद्मे. ततः किं. ततः किं. ततः किं.

Acknowledgements

The first name I must pay homage to is my advisor and mentor, Mamoun M.
Alhamadsheh. When I first walked into his PharmD biochemistry course as a pharmacy
freshman, I remember sitting in the back of the Rotunda with friends, and having zero intent on
paying attention. Within the course of that 2-hour lecture, the man had somehow enamored me. I
could see the passion with which a true scientist talked about his life's work. I wanted that
passion.

Fast forward a few years, he was more than supportive in allowing me to join his lab. I
still remember the day I started my PhD, while patting my shoulder he said "you will look back
on this day with extreme emotion. Time will tell whether that emotion is hatred or love." I am
paraphrasing, but the message was clear, the road ahead will be tough but fulfilling. I think I
have my answer to that question. Joining the Alhamadsheh lab was one of the biggest blessings I
could have received from the universe. I cannot imagine getting the blend of support and
challenge anywhere else. Even now as I type this at the end of my journey, in the middle a
November night, I look back on that day with humility and gratitude. Ironically Dr. Al will be
getting a copy of this dissertation to look over when he wakes up at 4 AM, in a few hours, to
review this document. That is the best way to understand the commitment with which he
supports his students. He doesn't act like an advisor; he acts like family. He will yell at you like
an older brother when you need it, and then coddle you like an older sister with jokes and food.

Dr. Al, I thank you from the bottom of my heart for every single lesson you taught me in
these years. You gave me challenges when I was hungry and had my back when those challenges
got the better of me. From personally delivering food to my apartment when I was sick, to

talking to me at 8 AM on a Sunday after my experiments gave "interesting" results; I thank you. I have never seen any boss act with such love and goodwill. I can never forget the man who made me into whatever the future holds for me. I hope I do you proud, sir.

I also must thank Dr. William Chan for being generous enough to open his lab doors to me as a Pharmacy student, and who again welcomed me during the Interleukin project. I remember asking him so many questions to the point where even I'd feel bad for asking. Despite this, I never saw even an inkling of annoyance on his face. To this day, I don't understand the level of generosity his heart holds for teaching students. Like Dr. Al, he too supported me greatly during the challenging times of the IL-2 project. I cannot forget how he taught me even the most basic molecular biology techniques with great patience and inspired me to always think on how I can improve my experiments.

Finally, I must thank my parents. I do not have the words, nor the intellect, to recount the blessings I was given for having such parents. Through thick and thin, good and bad, they have always found a way to make me smile. Regardless of how their life was, and what stress they had to endure, they acted as steadfast anchors for me. I would be a fool to even attempt any further depiction of the infinitude of love in their hearts for me. It is my sincere hope, that one day I will be the reason they hold their heads high with pride and joy.

Love, your little tiger.

-Arjun.

Enhancing half-life of Interleukin 2 by conjugation to the Transthyretin Ligand, TLHE

Abstract

By Arjun D Patel

University of the Pacific

2023

The central dogma of biology states that genetic information describes the flow of information from DNA to RNA and then finally resting in proteins. The fundamental aspect that underlies all aspects of life is the expression and modification of proteins. One can even argue that there is no life without proteins. As such, many human diseases are either directly or indirectly related to dysfunction of proteins and can potentially be solved through protein therapeutics. Consequently, scientists have begun to harness the diversity of proteins to treat the diseases which plague man in the form of protein therapeutics such as clotting factors, cytokines, and growth factors. Unfortunately, the short circulation half-life of proteins is a major limiting factor which must be overcome before their widespread adoption as a platform for therapeutic development. Contributing factors to this short circulation half-life include renal elimination, proteasomal degradation, and metabolism in the liver. Namely, renal elimination is the main challenge for protein therapeutics and warrants clinicians to resort to higher doses and more frequent administrations to maintain necessary concentrations in the body. Unfortunately, side effects of this approach are dose limiting toxicities and reduced therapeutic outcomes as drug concentrations fluctuate drastically. As a result, addressing the challenge of renal elimination for protein therapeutics would allow for the development of novel treatments which were previously not viable.

The human glomerulus readily filters out any particle smaller than approximately 30 kDa in weight. As a result, strategies adopted all share a common theme of endowing the protein with a greater effective size without compromising their natural activity against the intended target. The current approaches include conjugation to a polymer (i.e., PEGylation), covalent or non-covalent binding to a larger protein, or conjugating to the neonatal Fc receptor. Major limitations of these approaches include compromised activity caused by steric hinderance rooted in conjugation to moieties of larger size. This issue applies to all of the aforementioned reported approaches wherein activity becomes reduced, thus necessitating higher dosages. Furthermore, other limitations also exist such as humoral immune responses against polymers through anti-PEG antibodies, occurrence of organ damage, and solubility issues.

A novel approach was recently developed by the Alhamadsheh lab which demonstrated the ability of a small molecule linker termed "Transthyretin Ligand for Half-life Extension" (TLHE) to extend the circulation half-life of Gonadotropin releasing hormone. Most essentially, this was accomplished without compromising the potency or introducing a major sterically bulky group to the original peptide. Furthermore, additional concerns such as solubility issues was demonstrated to not be an issue either.

In this work, human Interleukin-2 (IL-2) was chosen as a proof of concept to demonstrate application of the TLHE technology in a protein to address the aforementioned half-life challenge. Previously, a mixture of IL-2 and TLHE-IL-2 was demonstrated to maintain comparable activity to control IL-2 in both in vitro and ex vivo efficacy assays. Furthermore, a pharmacokinetic evaluation in rodents demonstrated significant half-life extension of TLHE-IL-2. The objective of this work was to shift the ratio of the IL-2/TLHE-IL-2 mixture to majority TLHE-IL-2 and or enhance the yield of the mixture for further in vivo efficacy evaluation.

Table of Contents

List of Figures

Figure

List of Schemes

Scheme

List of Abbreviations

IL-2   Interleukin-2

IV   Intravenously

SC   Subcutaneously

PEG   Polyethylene Glycol

TLHE   Transthyretin Ligand for Half-life Extension

TTR   Transthyretin

kDa   Kilodaltons

LC-MS/MS   Liquid Chromatography- Mass spectrometry-mass spectrometry

RBP   Retinol Binding Protein

T4   Thyroxine

Fmoc   fluorenylmethoxycarbonyl protecting group

DIC   N,N′-Diisopropylcarbodiimide

HOAt   1-Hydroxy-7-azabenzotriazole

HATU   Hexafluorophosphate Azabenzotriazole Tetramethyl Uronium

TFA   Trifluoroacetic Acid

TIPS   Triisopropyl Silane

CHAPTER 1: ENHANCING THE HALF-LIFE OF INTERLEUKIN 2 BY
CONJUGATION TO THE TRANSTHYRETIN LIGAND, TLHE

Introduction

What Are Protein Therapeutics?

Protein therapeutics is an umbrella term used to describe any protein-based treatment used to favorably alter the pathophysiology of a disease state. The first demonstration of this was seen in the utilization of the protein Insulin in the treatment of Diabetes Miletus to compensate for diminished endogenous secretion of Insulin via pancreatic β-cells in the Isles of Langerhans[1]. To date, there have been more than 200 protein therapeutics which have been approved for use in the treatment of diseases[2]. These protein-based therapeutics hold many advantages when compared to conventional small molecule-based therapies. Inherently, proteins are able to mimic the complexities of drug targets better than small molecules which afford less off target activity and enhanced selectivity[1]. Unfortunately, these benefits are offset by one major challenge, their short circulation half-life. This short half-life is attributed to small proteins being readily filtered by the glomerulus, liver metabolism, and immunogenicity[3]. The main exception to this short circulation half-life due to small size dilemma are antibody-based therapeutics[3]. However not all therapeutic proteins are able to exhibit such large size, and most protein therapeutics are eliminated from the body very quickly.

As a bypass, clinicians have been forced to dose these drugs more frequently and at higher doses[4]. This more intense dosing regimen leads to ever fluctuating concentrations and higher initial concentrations to compensate for the impending sharp concentration drop-off [4]. Considering that many protein therapeutics are highly potent and can exhibit narrow therapeutic indexes, the combination of frequent large doses and narrow therapeutic windows leads to

serious side effects for patients. Consequently, this forces clinicians to sometimes skip doses, resulting in unfavorable therapeutic outcomes[4]. Furthermore, these issues weigh heavily on quality-of-life outcomes for patients as these therapies are administered either intravenously (IV) or subcutaneously (SC). As a result, patients are forced to come into clinical settings more frequently and experience greater levels of pain and discomfort which further compounds their suffering and increases healthcare costs. Thus, there is a great need to create a technology which can elongate the half-life of potential protein therapeutics without compromising their native pharmacodynamic properties.

Current Strategies Addressing Short Circulation Half-life

There are a few notable strategies to extend circulation half-life for proteins: polymer conjugation, albumin binding (covalent or noncovalent), and fusion with the Fc fragment of antibodies (Figure 1).

Figure 1

Half-life Extension Strategies[3]
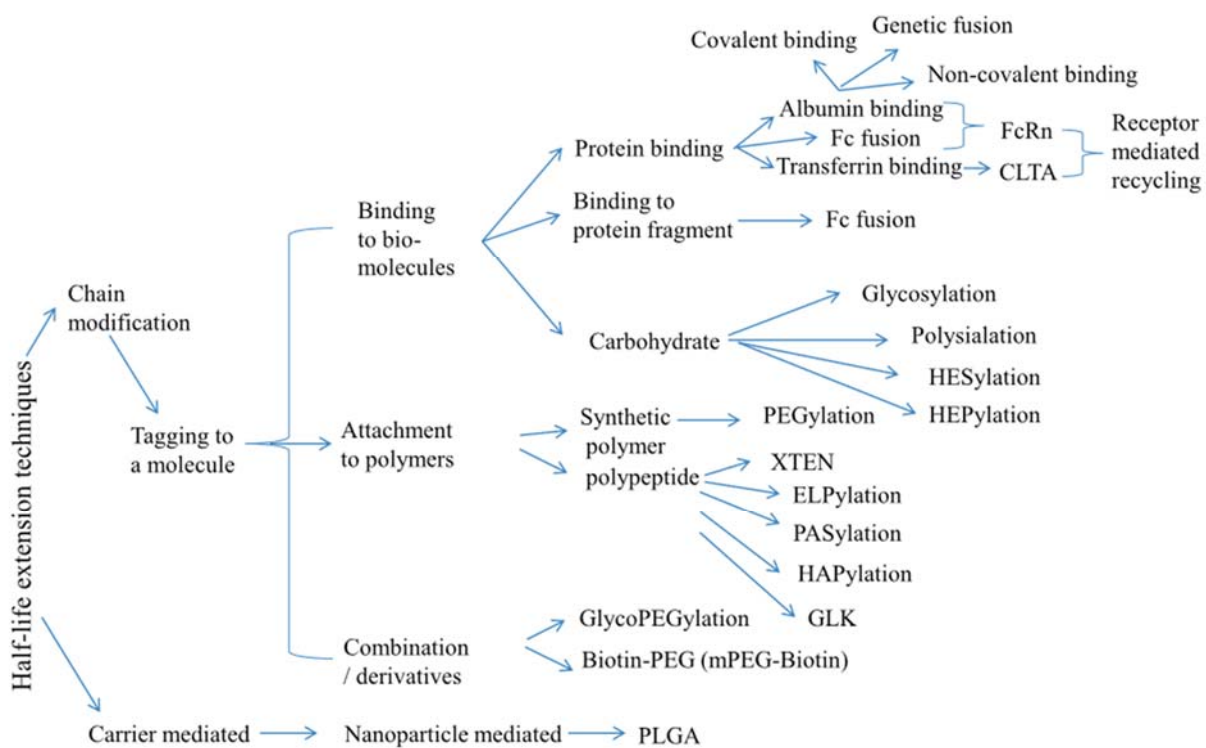
Polymer Conjugation/PEGylation

Covalent linkage of small proteins to polymers such as Polyethylene Glycol (PEG) is a concept introduced more than 50 years ago by David and colleagues[37]. Currently, there are more than 20 PEGylated macromolecular drug products available, making it one of the most common methods employed to prolong half-life for small proteins (Figure 2).

Figure 2

Table of Pegylated Approved Products[3]

Protein therapeutics	Plasma half-life	PEGylated formulations (patent name)	Plasma half-life	animal model/pre-/clinical trial	Ref.
Filgrastim recombinant human granulocyte colony-stimulating factor (G-CSF) (rmetHuG-CSF)	3.5–3.8 h	Pegfilgrastim (PEG-rmetHuG-CSF, Neulasta®)	42 h	In market	[5,17,19]
Recombinant factor VIII	12 h	Adynovate (PEG-FVIII)	13.4–14.7 h	In market	[13,20]
Recombinant factor VIII	12 h	BAY94–9027	19 h	PhaseIII	[13,20]
Enzyme adenosine deaminase (ADA)	few min	Adagen®Pegademase bovine	48-72 h; 3-6 dys	In market	[15,21,22]
ʟ-asparaginase	34 ± 8 h	PEGylated ʟ-asparaginase (Oncaspar®; Enzon)	357 ± 243 h	In market	[21,23,24]
Erythropoietin	> 24 h	Mycera®	142 h	In market	[5,25,26]
alfa-2a	5 h	PEGASYS (Roche)	160 h	In market	[16,21,24,27]
alfa-2b	2.3 h	PegIntron	4.6 h	In market	[24,28]
Erythropoietin mimicking novel protein	......	Peginastide (brand name: Hematide/Omontys)	21.5 h 59.7 h	In market	[16,24]
Synthetic integrin-binding peptide	28 min	HM3	162 min	rat	[16]
Recombinant growth hormone (GH)	4–5 min	NNC126–0083 (Novo Nordisk)	47.6 h	Phase I	[7,29–31]
GH	4–5 min	Somavert/ pegvisomant	6 days	In market	[24,30–32]
GLP-1	2 min	PEG- biotinylated GLP-1 (DBP-GLP-1)	Elongated half-life. Activity for 3 h	preclinical	[7,33]
Rasburicase (recombinant) Urate oxidase	8 h	Krystexxa	10–12 dys; application just once every 2 to 4 wks	In market	[24,34]
Tumour necrosis factor receptor type I	.....	r-Hu-sTNF-RI	3–29 h	Preclinical: Chimpanzee	[35]

The process of conjugating proteins with PEG results in an increase in their hydrodynamic size, thereby leading to a reduction in glomerular filtration inside the kidneys. The incorporation of a hydrophilic PEG moiety can provide protection for proteins against proteolysis. This protection is achieved by the creation of steric hindrance, which effectively obstructs the proteolytic substrate domain of the protein. Conjugation to PEG and other similar polymers can be categorized into two domains, nonspecific and site-specific conjugation. Nonspecific PEGylation can be achieved by using the available free amino groups present on proteins, namely lysine side chains and N-terminal amino groups. Site-specific coupling can also be accomplished by utilizing the sulfhydryl groups derived from cysteine residues that are accessible or groups that are introduced via genetic engineering techniques, or the N-terminal amino group if that can be selectively targeted depending on other residues in the primary structure. From the polymer side, PEG polymers can be produced in the form of linear or branched chains. Furthermore, these polymers can be designed to include reactive functional

groups such succinimidyl esters, aldehydes, or maleimide groups at their ends as sites of conjugation. These functional groups enable a range of conjugation techniques to be employed in the final goal of increasing hydrodynamic size. As a result, PEGylation presents a dynamic approach, capable of prolonging circulation half-life of proteins.

Notwithstanding the benefits afforded by PEGylation, it is imperative to consider several limiting factors associated with this approach including formation of organ damage, immunogenicity, and compromised potency. Firstly, at elevated concentrations and repeated exposures, PEG has the potential to induce organ damage in a myriad of tissues including the choroid plexus, kidneys, and other tissues with epithelial lining. The aforementioned outcome can be attributed to the non-biodegradable nature of PEG, which is primarily eliminated by the kidneys without undergoing any significant changes[5]. Next, generation of targeted antibodies against PEG polymers has been observed in human subjects subsequent to exposure with PEG-conjugated medications[6]. Furthermore, pre-existing anti-PEG antibodies have been detected in more than a quarter of the general population, leading to faster elimination of PEG-conjugated agents and presents an added layer of uncertainty[7]. Lastly, PEGylation has been demonstrated to diminish potency in the new conjugate[8]. This drop is primarily attributed to the contact between the PEG chain and the target leading to a steric blockage between the protein binding interface and its target receptor[8].

Albumin Binding & Fusion

Scientists have also employed the abundant plasma protein, albumin, as a carrier in order to extend the circulation half-life of therapeutic proteins. With a molecular weight of around 66 kilodaltons (kDa), the size of albumin is significant enough to prevent it from being easily filtered by the glomerular filtration process. In addition, it is worth noting that albumin

constitutes roughly 60% of the total blood proteins, with a concentration that falls within the range of 35-50 g/L. It is synthesized inside hepatocytes and subsequently secreted into the portal vasculature, with a production rate ranging from 9 to 12 grams per day. The primary role of albumin is to act as a transporter for a diverse range of hydrophobic substances, which can originate from both internal and external sources. The transported entities encompass a variety of substances, including as hormones, fatty acids (FA), hydrophobic medicines, and other compounds. The extended duration of albumin's presence in the bloodstream, which spans around 19 days, can be ascribed to two primary reasons. The first notable characteristic is its capacity to evade glomerular excretion, while another is its capability to undergo recycling through interactions with the neonatal Fc receptor (FcRn). It is worth mentioning that there are mainly two techniques employed to harness the ability of albumin to extend the half-life of drugs: covalent attachment and non-covalent attachment (Figure 3).

A proven method of covalent attachment is albumin fusion which involves the genetic fusion of the protein therapeutic gene with the albumin gene. Subsequently, the fusion gene is introduced into an appropriate host organism and expressed to obtain the new fusion protein. The initial manifestation of this methodology was shown by the approval of albiglutide, a peptide agonist of GLP genetically linked with human albumin. The albumin fused GLP peptide agonist was determined to have a half-life ranging from 6 to 8 days, allowing practitioners the convenience of administering the medication once a week.

The GLP arena has also seen the emergence of liraglutide, which offers a well-established approach to non-covalent attachment (Figure 3). In this product, researchers employed the conjugation of an analog GLP peptide with a C16 long chain fatty di-acid in order to extend the duration of circulation half-life. Their technique involves using long chain fatty acids as ligands

for endogenous human albumin, which naturally functions as a carrier for fatty acids. Consequently, the half-life was prolonged and was able to provide patients with the ability to take daily doses. Following further optimization of the long chain fatty acid constituent, Semaglutide was developed with an extended fatty acid chain and an increased circulation half-life, enabling the administration of a single weekly dose. Currently, the sole non-covalent albumin binders that have received approval are fatty acid conjugates, which have demonstrated a safe capacity to prolong the duration of circulation half-life. Regrettably, this particular method is also accompanied by a significant limitation, namely solubility. As a result, these fatty acid conjugates were categorized as BCS class IV, indicating their limited solubility and permeability. BCS is a classification used to categorize medications based on their dissolution, aqueous solubility, ability to permeate intestinal barriers[38]. The limited solubility for the fatty acid-GLP example was not considered significant due to the intrinsic potency provided by the GLP agonist peptides. However, in the case of other applications where bigger dosages are necessary, the restrictions in solubility that come with the fatty acid method present a substantial obstacle to the advancement of further development.

Figure 3

Various approaches employed to harness albumin to extend half-life[3]
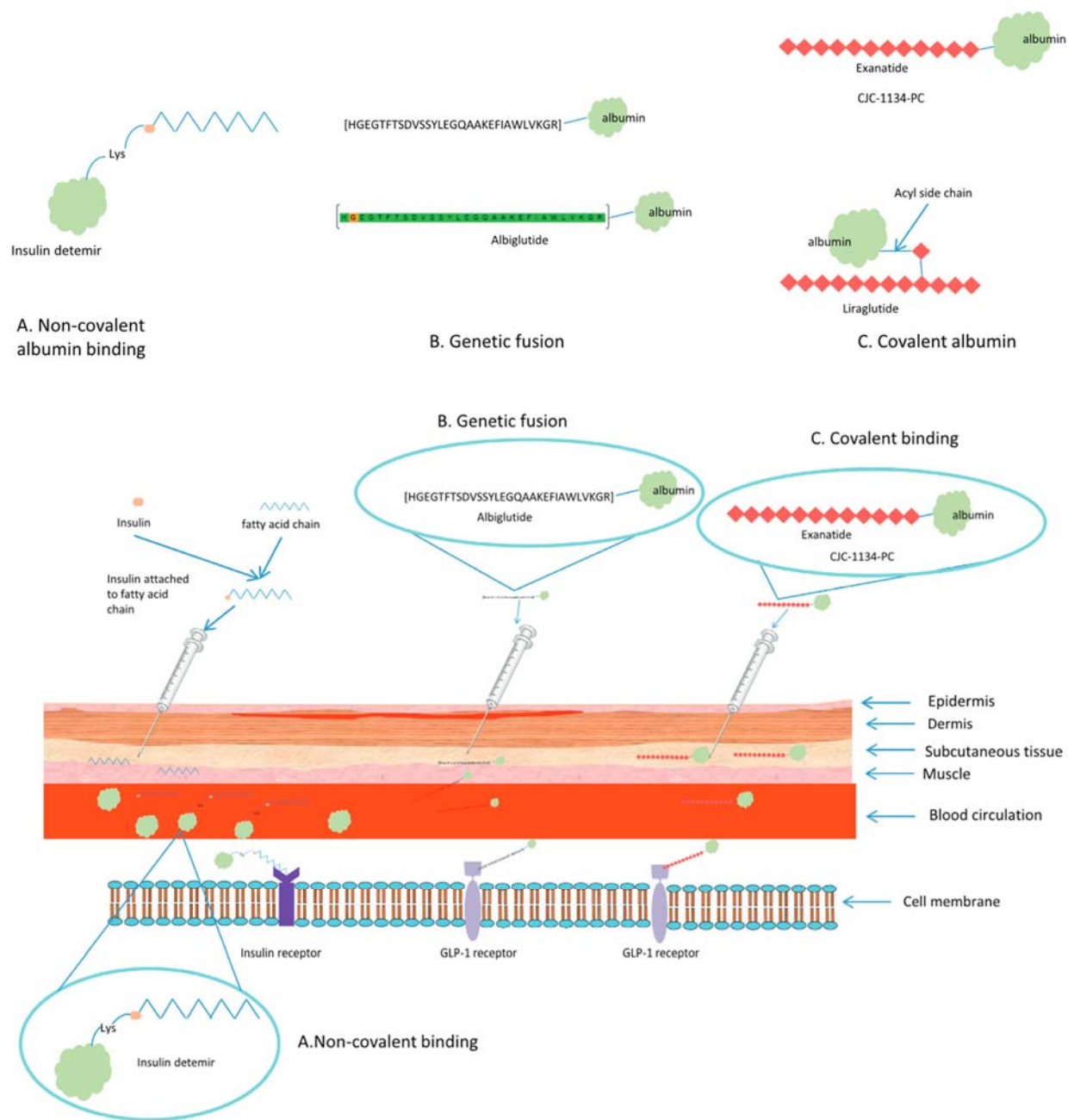
Fusion To Fc Fragment of Ig (Immunoglobulin)

The utilization of the Fc fragment of Ig (immunoglobulin) has been proven in yet another GLP drug named dulaglutide. This product includes an analog GLP peptide agonist genetically fused with the Ig fragment of human IgG4. As a result of this, improved outcomes in terms of solubility, immunogenicity, and circulation half-life were observed[9]. Nevertheless, it is important to acknowledge the presence of certain limitations associated with this particular methodology. Specifically, the presence of a significant sterically bulky Fc fragment which can cause a decrease in intrinsic potency of the original entity, thereby affecting the broader efficacy of the strategy[10].

Transthyretin

Transthyretin (TTR) or Prealbumin, initially identified in 1942, is a plasma protein with a molecular weight of 56 kDa[11]. It exists as a homo-tetramer in structure[11,12]. The production of this protein is predominantly carried out by the liver and then released into the bloodstream, resulting in a plasma concentration ranging from 0.2 to 0.4 mg/mL[11]. Additionally, it is possible for it to be produced inside the choroid plexus and be subsequently discharged into the cerebrospinal fluid (CSF), where its concentration typically falls within the range of 0.02–0.04 mg/mL[12]. In addition to its synthesis in the liver and choroid plexus, transthyretin (TTR) may also be generated in several other tissues, including the retinal pigment epithelium of the eye, the islets of Langerhans in the pancreas, the gut, and the meninges, albeit in minimal quantities[11]. The primary function of TTR is to serve as a supplementary transporter of thyroxine (T4) and the principal transporter of holo (containing retinol) retinol-binding protein (RBP). The half-life of human transthyretin (TTR) is around two days, with the liver, muscle, and skin serving as the primary locations for TTR breakdown.

TTR Structure

The determination of the structure of wild-type (WT) TTR in humans was accomplished in 1978 by the utilization of X-ray diffraction analysis, yielding a resolution of 1.8 Å[14]. At present, the Protein Data Bank (PDB, www.rcsb.org) has recorded over 200 crystal structures of wild-type (WT) or mutant transthyretin (TTR) derived from several species, including human, rat, mouse, chicken, and fish. In terms of its structure, each TTR monomer is composed of 127 amino acids, which come together to form eight β-strands, designated as A to H, as well as a single short α helix[15]. The dimerization process involves the interaction of two monomers, where the β-strand D-A-G-H from one monomer forms a T4 binding pocket with the corresponding β-strand from another monomer[14,15]. The T4 binding site may be subdivided into three distinct components, specifically designated as P1, P2, and P3.

The outermost section of the channel is comprised of P1, which is constituted of the side chains of Met13, Lys15, and Thr106[16]. P2 lies at the center of the channel, which exhibits mostly hydrophobic characteristics owing to the presence of hydrophobic side chains of Leu17, Ala109, and Leu110. The backbone carbonyl groups of Lysine 15, Alanine 108, and Alanine 109 residues is thought to introduce a degree of hydrophilicity to the P2 region[16,17]. The innermost region of the channel is identified as P3, which comprises the side chains of Ala108, Ala109, Leu110, Ser117, and Thr119. The hydrophilic component of P3 is derived from the side chains of Ser117 and Thr119, as well as the main chain carbonyl and amino groups of Ala108, Ala109, Leu110, and Thr118[16,17]. The TTR dimer has the capability to undergo assembly with another dimer, resulting in the formation of the TTR tetramer. This tetramer structure is characterized by the presence of two T4 binding pockets. The binding site of the holo-retinol-binding protein

(holo-RBP) on transthyretin (TTR) is situated in a perpendicular orientation to that of thyroxine (T4) [17].

Figure 4

Schematic model of TTR bound to T4 and holo-Retinol–binding protein (holo-RBP)[18]
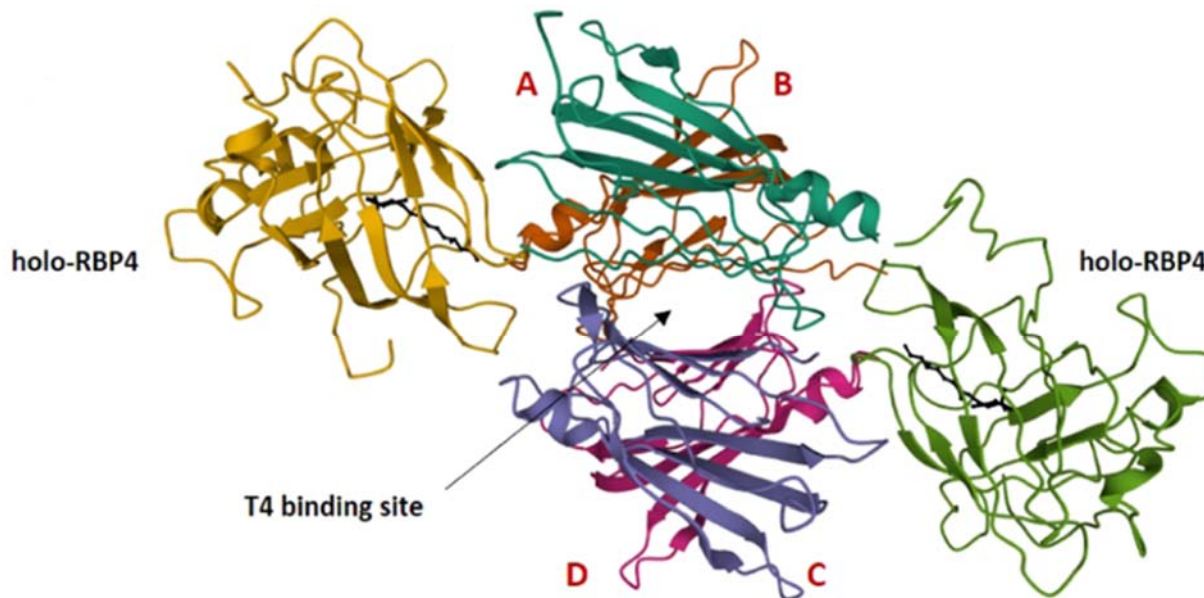
Role of TTR as a Transporter

Transthyretin is known to bind and transport two main moieties: Thyroxine (T4) and Retinol-Binding Protein (RBP). In view of T4 transportation within the human bloodstream, it is worth noting that TTR is not utilized as the principal transporter for T4. This is owed to the presence of alternative T4 transport proteins, such as thyroxine-binding globulin (TBG) and albumin[12]. As a consequence, the TTR T4 binding sites in humans predominantly stay vacant. Despite the presence of two T4 binding pockets within the TTR tetramer, only one T4 molecule can bind to TTR at any given moment due to the development of negative cooperativity between

the two binding pockets[39]. In order to facilitate the transportation of Retinol throughout the

bloodstream, Retinol-Binding Protein (RBP) initially forms a complex with Transthyretin (TTR)

to mitigate the process of renal clearance. The interaction between RBP and TTR leads to an

extended half-life in circulation of RBP, thereby leading to enhanced interactions and

transportation of Retinol[12]. In addition to its role as a transporter of T4 and RBP, transthyretin

(TTR) has been discovered to possess other functions as well such as proteolytic activity.

According to reports, there is evidence suggesting that TTR has the capability to cleave the C-

terminus of apoA-I. This cleavage process has been shown to diminish the capacity of apoA-I to

facilitate cholesterol efflux while also enhancing the amyloidogenicity of apoA-I. Consequently,

these molecular changes contribute to the progression of atherosclerosis[40].

Background on Interleukin-2 (IL-2)

The Biology of IL-2

Interleukin-2 (IL-2) is a cytokine with a molecular weight of around 16 kDa. It was

initially identified in 1976 as a growth factor for T cells, and was shown to be present in the

liquid supernatant portion of centrifuged mitogen-activated human T cells[25]. Interleukin-2 (IL-2)

is composed of four alpha helices and exerts its biological activity via interacting with several

IL-2 receptors (IL-2Rs). The IL-2 receptors can be categorized into three types based on their

structure: monomeric, dimeric, and trimeric IL-2 receptors (Figure 5). Monomeric interleukin-2

receptors (IL-2Rs) are composed of an α chain, which is also referred to as CD25 (IL-2Rα)[19].

The monomeric interleukin-2 receptors (IL-2Rs) have a binding affinity (Kd) of 10^{-8} M towards

interleukin-2 (IL-2), however this interaction between IL-2 and IL-2Rα does not elicit a

subsequent signal cascade response[19]. The β chain, also referred to as CD122, and the γ chain,

also known as CD132, combine to create the dimeric IL-2Rs[19]. The trimeric IL-2Rs, known as

the αβγ complex, are composed of these two chains. Both the dimeric and trimeric interleukin-2 receptors (IL-2Rs) are capable of initiating a downstream signaling cascade upon binding to interleukin-2 (IL-2). It is worth mentioning that CD122 is also a constituent of the IL-15 receptor (IL-15R)[26]. Similarly, CD132 is also common component across multiple other interleukin receptors, including IL-4, IL-7, IL-15, and IL-21 receptors. The trimeric IL-2 receptors exhibit a strong binding affinity towards IL-2, as shown by a low dissociation constant (Kd) of 10^{-11} M. On the other hand, the dimeric IL-2 receptors have a moderate binding affinity towards IL-2, with a Kd value of 10^{-9} M[19]. Upon activation of IL-2Rs, the IL-2 signal can be transduced through three main signaling pathways: (1) Janus kinase-signal transducer and activator of transcription (JAK-STAT), (2) phosphoinositide 3-kinase/protein kinase B/mammalian target of rapamycin (PI3K/Akt/mTOR), and (3) the mitogen activated protein kinase. Extracellular signal-regulated kinase (MAPK/ERK) pathway. The expression of dimeric IL-2 receptors may be observed on several immune cell types, including antigen-experienced CD8+ T cells, memory CD4+ T cells, natural killer (NK) cells, and naïve T cells. During the process of T cell receptor stimulation, active T cells have shown ability to temporarily increase the expression of CD25 and express more trimeric IL-2Rs. Furthermore, it has been observed that the trimeric IL-2 receptors are capable of being produced in a constitutive manner inside the CD4+ forkhead box p3 (Foxp3) +Treg cells that originate from the thymus. There have been reports indicating that certain non-immune cells, such as pulmonary endothelial cells, also have a low degree of trimeric IL-2Rs expression.

Figure 5

IL-2 Receptor structures[19]
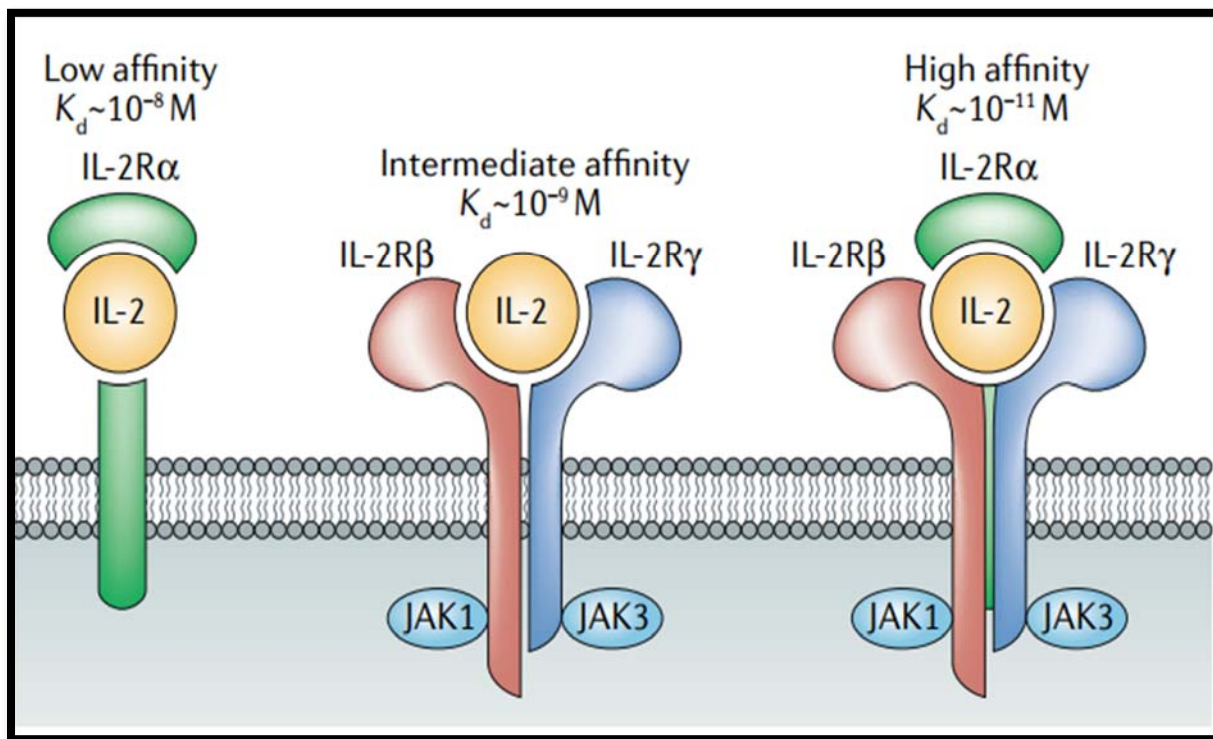
Interleukin-2 (IL-2) is primarily synthesized by activated CD4+ T cells, and to a lesser degree, by activated CD8+ T cells, activated dendritic cells, natural killer (NK) cells, and NKT cells. The entity in question possesses pleiotropic functions. T_{Reg} cells rely on it for their formation and homeostatic survival, hence contributing to the maintenance of peripheral immunological tolerance through the suppression of autoreactive effector T cells. In addition to its role in facilitating the activity of T_{Reg} cells, IL-2 also serves as a crucial factor in promoting the proliferation and differentiation of both CD4+ T cells and CD8+ T cells. Additionally, it has the potential to induce the proliferation of natural killer (NK) cells and enhance their cytotoxic activity and induce further generation of cytokines.

The Clinical Application of IL-2

The IL-2 therapy was granted approval by the US Food and Drug Administration in 1992 for the treatment of renal cell carcinoma, and in 1998 for the management of metastatic melanoma[20]. The recommended clinical dosage is documented as 600,000 International Units (IU)/kg (0.037 mg/kg). The recommended administration schedule for the dose is three times day, utilizing a 15-minute intravenous infusion. The treatment protocol consists of an initial phase of medication administration, succeeded by a period of 9 days of abstaining from medication, and subsequently followed by another phase of medication administration. The aforementioned pattern of alternating periods of rest and medication administration is continued unless any adverse effects that restrict the dosage are detected. These dosage limiting toxicities encompass severe life-threatening symptoms such as, vascular leak syndrome (VLS), hypotensive crises, abnormal respiratory patterns (hyper or hypoventilation), and fulfillment of systemic inflammatory response syndrome (SIRS) requirements[20]. Frequently, a significant number of patients experience challenges in adhering to prescribed dosage regimens due to the manifestation of dose limiting toxicities. Consequently, this phenomenon has a detrimental impact on treatment outcomes within clinical settings, resulting in fewer favorable results as can be seen in Figure 6. As a result, the utilization of IL-2 therapy is often limited to cases when other therapeutic options have been exhausted, namely for refractory malignancies that pose a significant risk of death.

Figure 6

Example of patient exhibiting hypotensive episodes during Aldesleukin (IL-2) therapy[20]
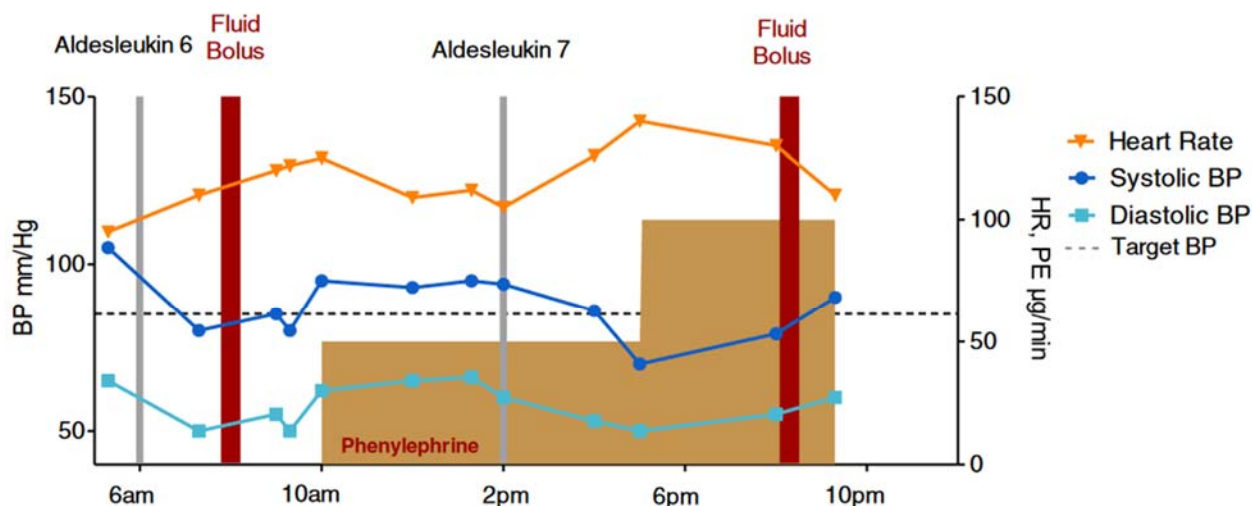
Figure 2 Timing of the administration of the 6th and 7th IV boluses of IL-2 is plotted versus systolic and diastolic blood pressure and heart rate. This patient is unresponsive to a fluid bolus and phenylephrine is begun at 50 mcg per minute with good effects permitting administration of the 7th dose. The resulting hypotension and tachycardia are treated with an increase in the phenylephrine dose and another bolus of fluid. The late night dose will likely be held.

Pharmacokinetics of IL-2

Interleukin-2 (IL-2) exhibits a notably short half-life inside the circulatory system. Following intravenous (IV) administration in mice, the observed serum half-life was determined to be 3.7 minutes[27]. In the human body, the levels of IL-2 exhibit a decline subsequent to an intravenous bolus injection. This decline is characterized by an initial half-life ranging from 5 to 7 minutes, followed by a terminal half-life spanning from 30 to 120 minutes. The kidneys serve as the primary location for the elimination of IL-2. The elimination of IL-2 begins with its filtration in the glomerulus of the kidneys, followed by its subsequent reabsorption in the cells of the proximal tubule, and ultimately its enzymatic digestion inside the renal tubules[27]. Cathepsin D is the renal protease accountable for the hydrolytic degradation of IL-2.

Expression Systems of IL-2

The utilization of the baculovirus expression system is a common approach employed for the production of recombinant proteins. After the gene of interest has been successfully inserted into the viral genome, the resulting recombinant virus may be replicated and isolated. These isolated recombinant viruses can then be employed to infect insect cell cultures, therefore facilitating the production of substantial quantities of the desired protein. The present baculovirus expression technique for the production and purification of recombinant human IL-2 is well developed. This technique of IL-2 expression developed by the K. Christopher Garcia group is widely recognized and esteemed in the academic community[27]. The researchers opted to insert the whole IL-2 gene sequence, together with a hexa-histidine tag at the C-terminus, into the pAcgp67A vector. The insect cells Spodoptera frugiperda (Sf9) were utilized to produce a recombinant virus with a high concentration, while Trichopulsia ni (High-Five®) cells were employed to express the resulting recombinant protein. The physiologically active recombinant human IL-2 has been successfully purified with the technique. The researchers have effectively acquired the crystal structure of IL-2 in conjunction with its receptor subunits. They have also assessed the binding affinity between IL-2 and its receptor subunits, and elucidated the mechanism by which IL-2 interacts to the receptor complex[27,28,29].

Since its initial replication in 1983, IL-2 has been extensively expressed via the E. coli expression method as well. In contrast to the baculovirus system, which yields properly folded and functionally active proteins, the E. coli method creates inclusion bodies (IBs) of IL-2[30,31].

Inclusion bodies, which are characterized as dense and insoluble particles, are known to occur within the cells of Escherichia coli. These entities arise as a result of the clustering of stable proteins inside the cytoplasm, exhibiting improper steric conformation and lacking the

intended biological functionalities[31]. The process of protein folding inside cellular systems is contingent upon the equilibrium established between the protein folding apparatus and the quality control mechanism. In a scenario of protein overexpression, whereby both the protein folding mechanism and quality control system exhibit reduced efficiency, the misfolded protein has the potential to combine and generate insoluble inclusion bodies. While soluble proteins are generally favored over insoluble inclusion bodies for the expression of recombinant proteins, the use of the E. coli expression system, which can produce inclusion bodies, remains prevalent in biopharmaceutical manufacturing[31]. This is likely attributed to the system's ability to achieve greater levels of protein expression compared to soluble proteins. In order to get the physiologically active protein from the inclusion body, it is necessary to carry out a procedure known as inclusion body refolding.

The initial stage of inclusion body refolding involves the liberation of the target protein from E. coli cells. Cell disruption can be accomplished by several methods such as sonication, French press, enzymatic treatment, or freeze-thawing of the cells[32]. Subsequently, the inclusion bodies may be isolated from cellular debris or other soluble contaminants using centrifugation or size-exclusion chromatography. The subsequent procedure involves the solubilization of the inclusion bodies, a task that can be accomplished by the addition of potent chaotropes such as 6 M guanidine hydrochloride or 8 M Urea[32]. In order to disrupt the disulfide bonds, a reducing agent, such as dithiothreitol (DTT), is used. The refolding phase is considered to be the most crucial stage in the process of inclusion body refolding. The objective of lowering the concentration of denaturants can be accomplished by a progressive process including dilution or dialysis.

One of the inherent difficulties associated with protein folding is in the inability to ascertain the precise proportion of proteins that successfully attain their appropriately folded conformation. Various techniques for the refolding of IL-2 in the E. coli system have been effectively employed by researchers, resulting in the production of physiologically active IL-2. Arkin et al., have shown that 8 M guanidine hydrochloride can be used to solubilize the inclusion bodies[33]. Subsequently, the solubilized substance underwent dialysis into a buffer solution consisting of 10 mM ammonium acetate and 25 mM sodium chloride (pH 6). Following this, the substance was subjected to further purification by chromatography using an S-sepharose column. The determination of the binding affinity to IL-2 receptors was conducted utilizing surface plasmon resonance (SPR) assay. Goodson and Katre resuspended inclusion bodies in a solution comprising 50 mM Tris, pH 8.0, with 8 M guanidine HCl, 100 mM DTT, and 25 mM EDTA, resulting in a final concentration of approximately 30 mg/mL. The solubilized substance underwent a heating process at a temperature of 40 °C for a duration of 15 minutes in order to achieve complete reduction of the cys3 rIL-2. Subsequently, it was subjected to dialysis using a solution consisting of 6 M guanidine HCI, 50 mM sodium acetate (pH of 5.5), 5 mM EDTA, and 10 mM DTT. Finally, the dialyzed sample was gradually diluted under a nitrogen environment using a solution containing 50 mM sodium acetate at pH 5.5 and 5 mM EDTA (pH 5.5), until reaching a concentration of 3 M guanidine HCI[34]. Malcolm P. Weir et al. solubilized inclusion bodies with a solution containing 6 M-guanidinium chloride and 10 mM-dithiothreitol (pH 8.5). Subsequently, the dissolved inclusion bodies were purified in a reduced and denatured state using gel-permeation chromatography in the aforementioned solvent. One notable method for refolding and purifying recombinant human interleukin-2, as demonstrated by the research group led by Koichi Kato, involves the utilization of cation exchange chromatography and reversed-phase

high-performance liquid chromatography (RP-HPLC)[36]. This approach specifically targets the recombinant protein generated in E. coli. The elution process in the reversed-phase high-performance liquid chromatography (RP-HPLC) was carried out using a linear gradient of acetonitrile concentration while including 0.1% trifluoroacetic acid (TFA). Typically, the use of organic solvents, such as acetonitrile, leads to the denaturation of isolated proteins. Notwithstanding the elevated concentration of acetonitrile employed for protein elution, the eluent IL-2 was able to maintain intact functionality as per their activity evaluation. The in vitro biological activity of the isolated protein was assessed based on its capacity to sustain NKC3 cells. The EC50 value that was determined through experimentation ranged from 36,000 to 40,000 U/mg. This range aligns with the established range of natural human IL-2, which is often reported as 23,000 to 46,000 U/mg of protein. The mechanism by which IL-2 retains its action when utilizing organic solvents as the elution buffer has not yet been fully elucidated.

Dissertation Objective (IL-2 Chapter)

Our lab has reported that the conjugation of IL-2 to a small molecule reversible binder of transthyretin (TLHE) can effectively prolong their circulation half-life of the TLHE-IL-2 conjugate. Unfortunately, the conjugation efficiency was not complete resulting in a ~1:1 mixture of the desired TLHE-IL-2 conjugate and unreacted IL-2. We have further demonstrated that mixtures containing TLHE-IL-2 and IL-2 result in an extended circulatory half-life while maintaining potency in vitro and ex vivo. Our hypothesis posits that enhancing the conjugation efficiency will result in higher ratio of the TLHE-IL-2 conjugate, which will result in larger extension in the in vivo half-life without substantial alterations in potency. One further secondary hypothesis posits that the utilization of TTR to extend the circulatory half-life of IL-2 may result

in a boosted anti-cancer in vivo efficacy, as studied through in vivo tumor xenograft mouse models. To investigate these assumptions, the following objectives were pursued:

1. Ascertain the best reaction conditions for the conjugation of TLHE with IL-2, with a focus on achieving maximum uniformity and yield of TLHE-IL-2.

2. Employ several chromatographic techniques for the purpose of isolating TLHE-IL-2 from the conjugation mixture.

Outline of Proposed Studies

One of the aims of this work is to improve the uniformity and efficiency of the conjugation reaction between IL-2 and TLHE, with the goal of producing mixtures that are acceptable for potential in vivo pharmacokinetic and pharmacodynamic studies in the future. To accomplish this purpose, the inquiry will further explore the technique about the several factors implicated in the determination of reaction efficiency and yield.

Methods

Expressing IL-2 in E. coli

Expression and Storage of E. Coli Pellets

Previously, a batch of constructed pRSET A plasmid with a cDNA sequence to generate modified IL-2, was transformed into BL21(DE3) pLysS competent cells (Invitrogen, Catalog No. C606010) following the basic transformation procedure from the manufacturer. Then, 5ng of the expressed plasmid was transformed into One Shot® competent cells which then underwent heat shock for 30 seconds. Lastly, these competent cells were plated onto LB growth media with ampicillin and chloramphenicol.

Each time a batch of IL-2 was expressed, these cells were plated onto LB growth plates with ampicillin and chloramphenicol, and appropriate colonies were selected to inoculate 200

mL of LB broth also containing ampicillin and chloramphenicol. Ampicillin50 μg/mL (Gold Biotechnology, Catalog No. A-301-10) and 35 μg/mL Chloramphenicol (Alfa Aesar™, Catalog No. AAB2084114) were the final concentrations in both LB plates and LB broth media. Following incubation at 225 rpm for 12-16 hours at 37 °C, the incubated broth media (200 mL) was added into another 1L of fresh LB broth and an amount of IPTG was added to give a final 1 mM concentration. This 1.2 L of broth was incubated for another 6 hours at 225 rpm and 37 °C. Following the 6 hours of expression and incubation, the broth media was centrifuged for 16,000 rcf for 30 mins at 18ºC. After removing the supernatant, the pellet was resuspended in PBS with vigorous pipetting and then centrifuged again in the same manner. After discarding the supernatant, the pellets were stored in -80ºC.

Method of Refolding Expressed IL-2 in Inclusion Body

The finalized inclusion body refolding protocol to harvest and refold IL-2 from E. coli pellets is as follows. First, the E. coli pellet is sequentially thawed to room temperature, homogenized, and resuspended in PBS buffer followed by lysis via sonication. This suspension is then centrifuged for a duration of 30 minutes at a rotational speed of 16,000 g (rcf), while maintaining a temperature of 10 ºC. After discarding the supernatant, the resulting inclusion body pellet is resuspended in a solubilization buffer composed of 6 M Guanidine HCl, 100 mM Tris, 300 mM NaCl (pH 8). This mixture was again centrifuged the same as before and the supernatant denatured IL-2 is then added dropwise into a redox buffer (1.1 M Guanidine HCl, 100 mM Tris/ 6.5 mM cysteamine/ 0.65 mM cystamine/ pH 8) for refolding. After stirring at room temperature for four hours, the solution is centrifuged for a duration of 30 minutes at a rotational speed of 16,000 g (rcf) while maintaining a temperature of 10 ºC. Next, the supernatant is transferred into a 4 ºC environment and dialyzed for 12 hours against the

following buffer: 10 mM Ammonium Acetate (pH 6.5). All dialysis procedures were done using

SnakeSkin Dialysis Tubing (MWCO 3,500 Da). Lastly, the dialysate is again centrifuged as

before for a duration of 30 minutes at a rotational speed of 16,000 g (rcf), while maintaining a

temperature of 4ºC. The supernatant was then loaded onto a pre-equilibrated Cobalt-immobilized

resin (Gold Biotechnology; catalog no. H-310- 100) for metal-affinity chromatography. The

enriched protein fractions were eluted with the elution buffer (10mM Ammonium Acetate, 500

mM imidazole, pH 6.5). Lastly, the purified protein was dialyzed for 12 hours) against 10 mM

Ammonium Acetate, pH 6.5 buffer and centrifuged followed by evaluation by SDS PAGE and

BCA assay.

Conjugation Reaction Studies

The conjugation reaction between TLHE and IL-2 was previously conducted using a 6-

fold molar excess of TLHE linker to IL-2 in a 10 mM Ammonium Acetate buffer (pH of 6.5).

The final concentration of DMSO in the reaction mixture was 1%. The experiment started by

allowing pre-aliquoted IL-2 at a concentration of 1 mg/mL to thaw on ice, followed by the

addition of a TLHE linker stock under Argon atmosphere. The mixture was then gently pipetted

multiple times to ensure homogeneity. In cases when the necessary final concentration of

dimethyl sulfoxide (DMSO) exceeded the quantity achieved by adding the TLHE linker stock,

the relevant volume of DMSO was initially pipetted into the thawed IL-2 sample and carefully

mixed. Following that, the TLHE linker stock was introduced and well mixed to commence the

reaction. The reaction was monitored by the acquisition of small volumes of 10 μL each. These

samples were subsequently combined with 10 μL of 2X Laemmli Sample Buffer containing β-

mercaptoethanol. The resulting mixture was then subjected to vortexing in order to achieve

homogenization. Subsequently, the samples were subjected to a temperature of 95 ºC for a

duration of 60 seconds, after which they were kept at room temperature until a volume of 10 µL of the neutralized sample is applied onto the gel. At each time point, the vial underwent centrifugation at room temperature, specifically at a speed of 16,000 revolutions per minute, for a duration of 5 minutes. Subsequently, a visual examination of the vial was conducted to assess the presence of any precipitation. In order to investigate different pH levels or alternative buffer systems, the utilization of an Amicon Ultra-15 device was employed according to the manufacturer's provided methodology, if buffer exchange was required for the experiment.

Separating TLHE-IL-2 Conjugate from Unreacted IL-2

Mini-whole Gel Eluter

A variety of techniques were employed in the endeavor to isolate TLHE-IL-2 from the unbound IL-2 present in the reaction mixture. The initial step was the use of the Mini Whole Gel Eluter, which was provided by BioRad. Subsequently, it was discovered that the Mini Whole Gel Eluter had become an unsupported device. As a result, an alternative device, the Model 422 Electro Eluter, was employed using a modified approach. Both techniques aim to isolate individual protein bands from gels of both acrylamide and agarose composition. By applying either technique, researchers have the capability to extract denatured protein from acrylamide gels in a manner that is perpendicular to their conventional direction of migration during electrophoresis. Consequently, it is possible to isolate specific protein bands within acrylamide gels. This approach can be particularly advantageous when the target protein band is in close proximity to an undesired band, and traditional gel-permeation chromatography methods are insufficient for isolating the desired protein band. In this particular scenario, where the disparity between the target protein band and the unmodified IL-2 band is minimal, owing to their size

discrepancy of less than 1 kilodalton (kDa) and minute differences in physiochemical

characteristics, the employment of the gel elution technique has considerable potential.

Figure 7

Graphic depicting Mini Whole Gel Eluter Apparatus. Zoomed elution chamber on right[21]
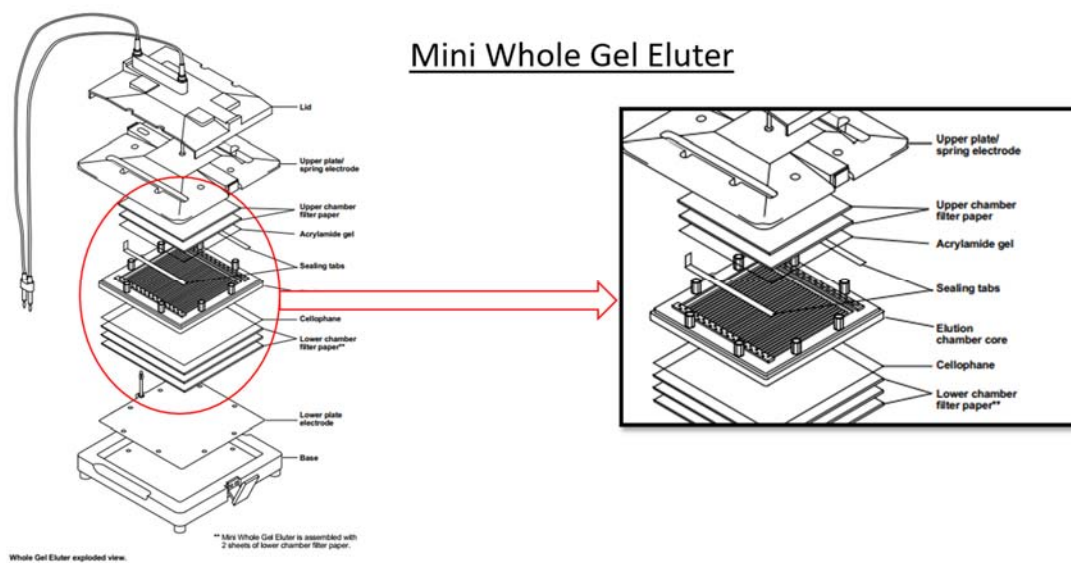
Model 422 Electro Eluter

Figure 8

Diagram illustrating the electrophoresis apparatus used to elute proteins from gel slices into the membrane cap chamber[22]
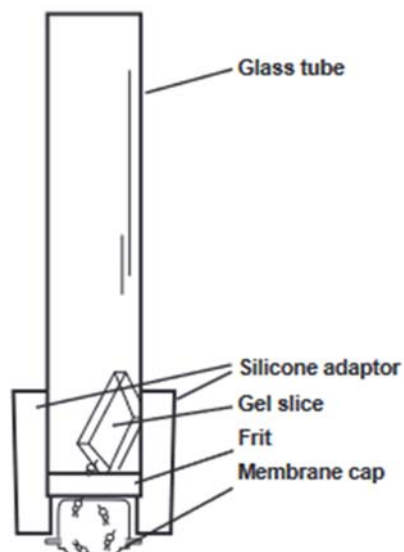
When comparing the Model 422 Electro Eluter (Figure 8) to the Mini Whole Gel Eluter (Figure 7), researchers are provided with a somewhat greater degree of flexibility in terms of selecting the specific bands that are to be isolated. The flexibility to isolate the protein band of interest is derived from the procedure employed, wherein the gel slices are physically dissected and separated prior to elution of the target protein. One notable distinction between the Mini Whole Gel Eluter, which required optimization for the Model 422 Electro Eluter, pertained to the staining and de-staining procedure employed for the gel.

Technical Challenge 1: Coomassie Stain. The Coomassie staining of the gels was

necessary in order to facilitate the cutting procedure with a heightened degree of accuracy, hence

minimizing the inadvertent inclusion of unreacted IL-2 bands. Subsequently, it was also

necessary to remove the staining from these gel slices prior to starting the gel elution process.

The inclusion of the de-stain phase was implemented subsequent to the first attempt to elute the

target gel where it was observed that the retrieved eluent exhibited a profound blue hue, which

was attributed to the electrostatic attachment of the Coomassie dye to the protein present in the

eluent. More specifically, the Coomassie dye possesses a net positive charge due to the presence

of a quaternary ammonium functional group in its chemical structure. It was postulated that this

association could also disrupt future protein refolding endeavors as well as disrupt the overall

negative charge of the SDS-TLHE-IL-2 complex which would interfere with the electrophoresis

process. This phenomenon occurs due to the binding of SDS to the eluent protein during elution

electrophoresis, resulting in the protein being coated with SDS. Consequently, this predicament

was resolved by the implementation of a procedure derived from an in-gel tryptic digest

approach, wherein a destain buffer was employed to displace the Coomassie dye. The underlying

process is hypothesized to include the displacement of the Coomassie dye cation from the

negatively charged SDS-coated protein complex by the bicarbonate anion. As a result, the

ammonium group forms an association with the protein complex coated with SDS, which has a

negative charge.

Technical Challenge 2: Post Elution Refolding. An additional obstacle which had to be

addressed was refolding of the protein subsequent to the elution procedure. The current situation

presents a quandary regarding the elution procedure, which is carried out within a buffer system

consisting of 8 M Urea in TGS buffer (comprising 25 mM Tris, 192 mM Glycine, 0.1% SDS, pH

8.3). On the other hand, the process of refolding IL-2 from its inclusion body state involves initiating the refolding process using 6 M Guanidine HCl, followed by dilution and the introduction of a redox system consisting of Cystamine and Cysteamine. If the eluent was directly dialyzed against 6 M Guanidine HCl, it was found that the SDS-protein complexes associated with Guanidine resulting in insoluble complexes of SDS-protein-Guanidine which then precipitated out of solution instantly. To address this issue, two distinct approaches were employed. The first objective was to endeavor the replication of a refolding technique utilizing Urea. The second approach involved utilizing a commercially available product from ThermoFischer Scientific, namely the Pierce™ Detergent Removal Column, which exhibited selectivity in binding and complexing with SDS. The resolution of this dilemma was of utmost importance, as the isolated desired conjugate would not be suitable for subsequent investigations due to its incorrect physiologically active conformation.

Urea Based Refold. To study the refolding of IL-2 by the utilization of Urea, the experiment involved the thawing of two E. Coli pellets containing expressed IL-2 inclusion bodies and trying to refold them as separate duplicate groups. This study design was done to prevent any false negatives where the reaction refolding failed because there was no IL-2 expressed in the pellet batch. These pellets were subsequently homogenized in PBS buffer with a Dounce homogenizer and subjected to sonication. The suspension was thereafter subjected to centrifugation for a duration of 30 minutes at a rotational speed of 16,000 g (rcf), while maintaining a temperature of 10ºC. The pellets obtained were subsequently resuspended and solubilized with a 6M Guanidine HCl buffer solution. The resultant mixture was then subjected to centrifugation to eliminate any cell debris that remained insoluble. The supernatants of both groups were subsequently subjected to dialysis against 8M Urea, 100 mM Tris, 192 mM Glycine

buffer (pH 8.3). This was very similar to that which was buffer employed for gel elution but notably without SDS.

For the 8M Urea group, the dialyzed volume was centrifuged and added into a larger volume of 2M Urea containing a similar refolding buffer as the control 6M Guanidine HCl group. The only difference between the refolding buffers for each group was the presence of 1.1M Guanidine HCl versus 2M Urea in each respective group. Aside from this difference in redox buffers, both groups underwent the same standard process previously described to obtain purified and biologically active protein.

Pierce ThermoFischer Detergent Removal Column. The second solution to the post elution refolding challenge was the utilization of a proprietary detergent removal resin which had been reported to be able to remove SDS from protein samples. Here, the eluted protein sample in 8M Urea-TGS buffer is loaded onto the resin per the manufacturer protocol and a similar 8M Urea buffer with only Tricine and Glycine is used for washing. This solution post SDS removal is then dialyzed against the aforementioned solubilization buffer containing 6M Guanidine HCl. The dialysate then undergoes the same standard refolding protocol already described. The yield and purity of this procedure was studied via SDS PAGE and BCA assay.

Results and Discussion

Conjugation Reaction Studies

Increasing Molar Equivalents of TLHE Linker in the Reaction

Our lab has shown earlier that the best conjugation outcome came with performing the reaction in 10 mM Ammonium Acetate (pH 6.5) using molar excess of 6 equivalents of the TLHE Maleimide linker group and leaving the vial at room temperature for 24 hours. It was theorized that if another 6 equivalents were added at T_{0hr}, then the likelihood of lysine side chain

amines undesirably conjugating to TLHE would be higher. Furthermore, it was known that the maleimide ring functional group located on the TLHE linker could hydrolyze over 24 hours in aqueous buffer, rendering it inactive to covalently conjugate with the desired Cys-3 of IL-2. Therefore, we hypothesized that by adding another 6 equivalents of TLHE linker in 1% DMSO, a low and constant TLHE presence could be established and provide selective conjugation without resulting unwanted side reactions with lysines. In addition, an added control group was included to account for the addition of another 1% of DMSO at the 22 hour mark. This time was chosen because it was a sufficient period for the original 6 equivalents of TLHE linker to have degraded and a further two hours of reaction time for the addition new 6 equivalents to have an effect. It was postulated that if no difference was seen, then more than two hours would be provided in a subsequent experiment for the added 6 equivalents to take effect. However, it was found that just an additional two hours with the new 6 equivalents was sufficient to shift the reaction towards unwanted lysine side reactions.

The Green diamonds in Figure 9 signify reference IL-2 from pre-aliquoted pooled batches which was run in duplicate in the gel. Blue diamonds are the control group of the previous best method for executing the conjugation reaction. This method involved thawing the pre-aliquoted vial of IL-2 and diluting to 1 mg/mL concentration with 10mM Ammonium Acetate buffer (pH 6.5). Next, the TLHE linker stock dissolved in DMSO was added to give a final concentration of 1% DMSO with 6 equivalents of linker. This addition occurred under Argon atmosphere and involved pipetting to homogenize at the end before being left on benchtop for 24 hours at room temperature. The first blue diamond is a sample from T_{0hr} and the second diamond is from T_{24hr}. The yellow diamond signifies the group which was the same as the blue diamond group until T_{22hr} when the group was split into two parts. The first part received another

1% DMSO as a control which can be seen in the yellow group. The second part received another 6 equivalents of linker which also added another 1% DMSO to the reaction vial which is shown by the red diamonds.

Figure 9

Adding more TLHE equivalents into conjugation reaction
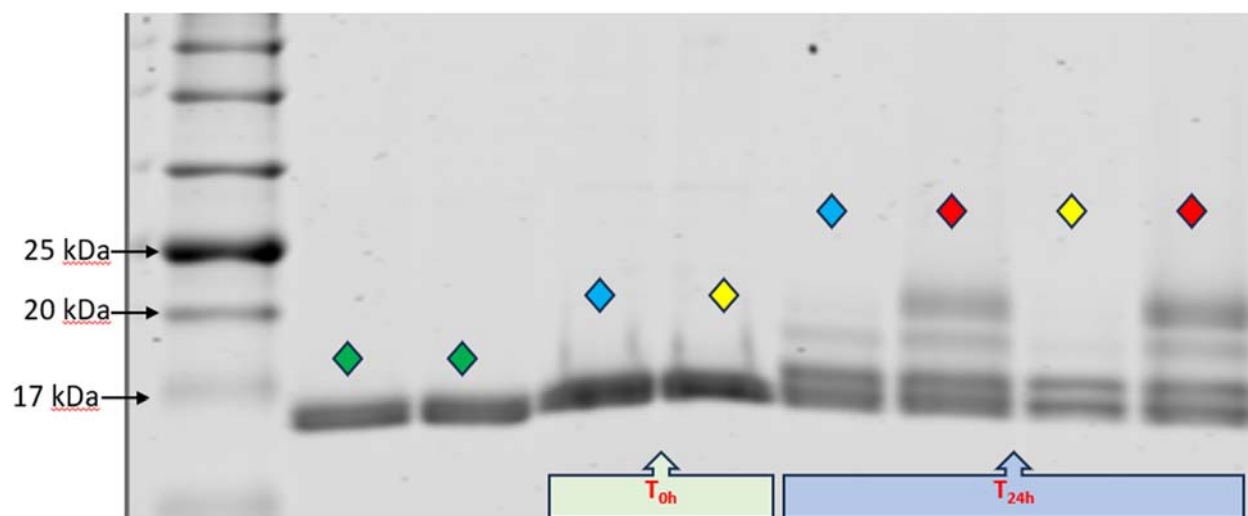
◆ Ref. IL-2

◆ 10mM Ammonium Acetate, 1% DMSO, 6 eq TLHE at T_{0h}, pH 6.5, RT. **(Previous Method)**

◇ 10mM Ammonium Acetate, 1% DMSO, 6 eq TLHE at T_{0h} + 1% DMSO (Ctrl) at T_{22h}, pH 6.5, RT.

◆ 10mM Ammonium Acetate, 1% DMSO, 6 eq TLHE at T_{0h} + 1% DMSO 6 eq TLHE at T_{22h} pH 6.5, RT.

Per the results, it was concluded that adding extra TLHE linker equivalents only served to increase undesired side reactions with the many lysine side chains of IL-2. Interestingly, it was observed that simply adding another 1% of DMSO to the reaction vial at T_{22hr} appeared to produce higher specificity above even the control blue diamond group. Due to this observation, it was decided that solubility of the linker will be further studied.

Optimizing TLHE-Linker Solubilization

Observing the 2% DMSO improve reaction outcomes, it was decided to further explore reaction conditions favorable for enhanced TLHE linker solubilization. In this experiment, the previous method which was described above was again used as a control (green diamond in Figure 10). Furthermore, the yellow diamond served as a replicate control for the 2% DMSO group wherein 6 equivalents of TLHE linker and the necessary additional DMSO was added to the reaction vial at T_{0hr} in order to maximize linker solubility. It was also theorized that the addition of glycerol could help stabilize IL-2 and improve its conformational stability. As a result, the hypothesis for this group was that additional solubilization of IL-2 with a glycerol co-solvent would perhaps better expose the Cys-3 group leading to more favorable reaction outcomes. Next, the red diamond group involved addition of 6 equivalents of TLHE, similar to the yellow diamond group, however with even more DMSO for a total of 4% DMSO at T_{0hr}. Lastly, it was also possible that the 10mM Ammonium Acetate buffer system (pH 6.5) itself was not appropriate for a conjugation reaction between IL-2 and the TLHE linker. The rationale being that Ammonium Acetate is not actually a true buffer system such as HEPES, and so there exists a possibility that the addition of even residual TFA from the TLHE purification process could acidify the reaction condition. Consequently, as the thiol maleimide reaction needs a specific 6.5-8 pH range to orthogonally work, a shift towards more acidic conditions could be what is preventing the reaction from progressing to completion.

Figure 10

Optimizing TLHE linker solubilization
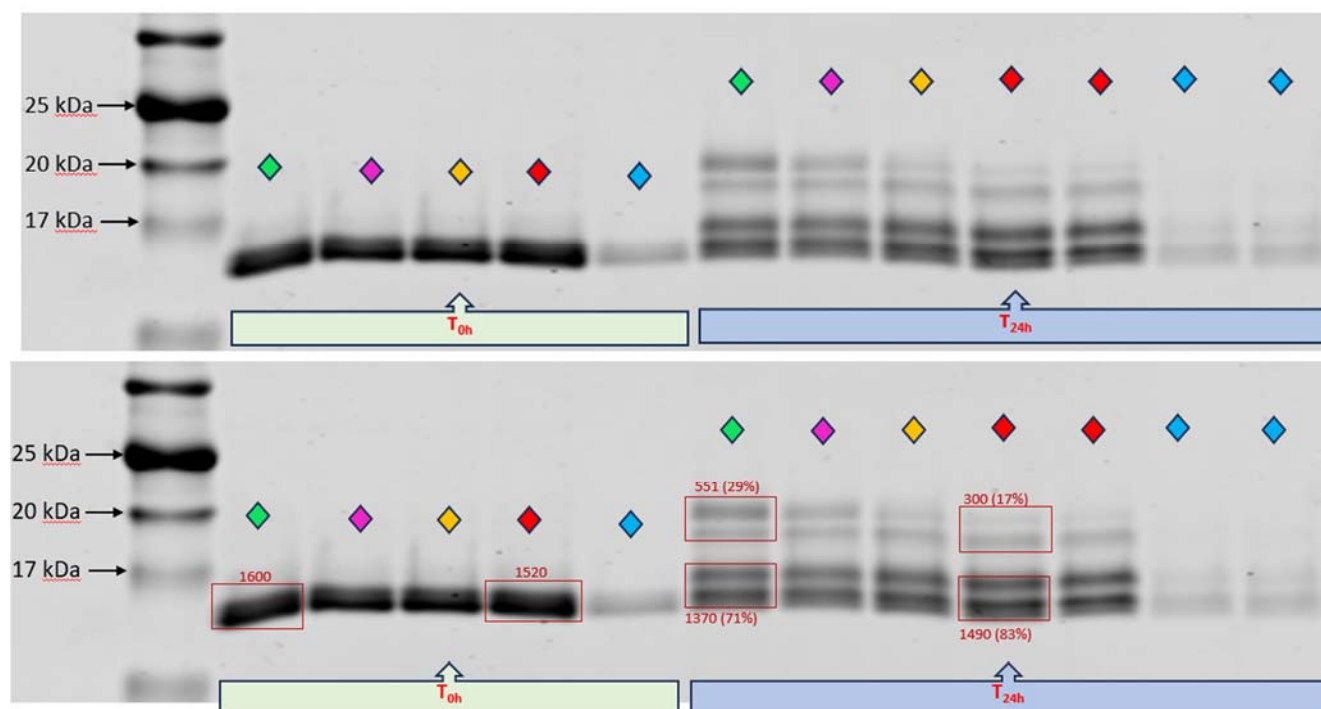
◆ Previous Method: 10mM Ammonium Acetate, 1% DMSO, 6 eq TLHE at T_{0h}, pH 6.5, RT

◆ 10% Glycerol, 10mM Ammonium Acetate, 1% DMSO, 6 eq TLHE at T_{0h}, pH 6.5, RT

◆ (Ctrl group): 10mM Ammonium Acetate, 2% DMSO, 6 eq TLHE at T_{0h}, pH 6.5, RT

◆ 10mM Ammonium Acetate, 4% DMSO, 6 eq TLHE at T_{0h}, pH 6.5, RT

◆ 100mM HEPES, 1% DMSO, 6 eq TLHE at T_{0h}, pH 7.5, RT

The takeaways from this experiment were that addition of glycerol did not appear to benefit reaction outcomes. Furthermore, the HEPES buffer system appeared to be unstable to IL-2. This instability was seen both at T_{0hr} but also further degradation occurred over the time course of the reaction. It was theorized that one reason for this phenomenon could be the higher concentration of HEPES at 100 mM causing a salt out effect for IL-2. The last conclusion which was drawn from this experiment was that the addition of 4% DMSO appeared to be the best at

solubilizing the linker as well as resulting in the least amount of Lysine side chain reactions. As a result, it was decided that subsequent experiments should continue with the best reaction condition benchmark to this point, 10 mM Ammonium Acetate with 4% DMSO (pH 6.5) containing only 6 equivalents of the TLHE maleimide linker introduced at T_{0hr}.

Figure 11

Observering IL-2 degradation in HEPES buffer
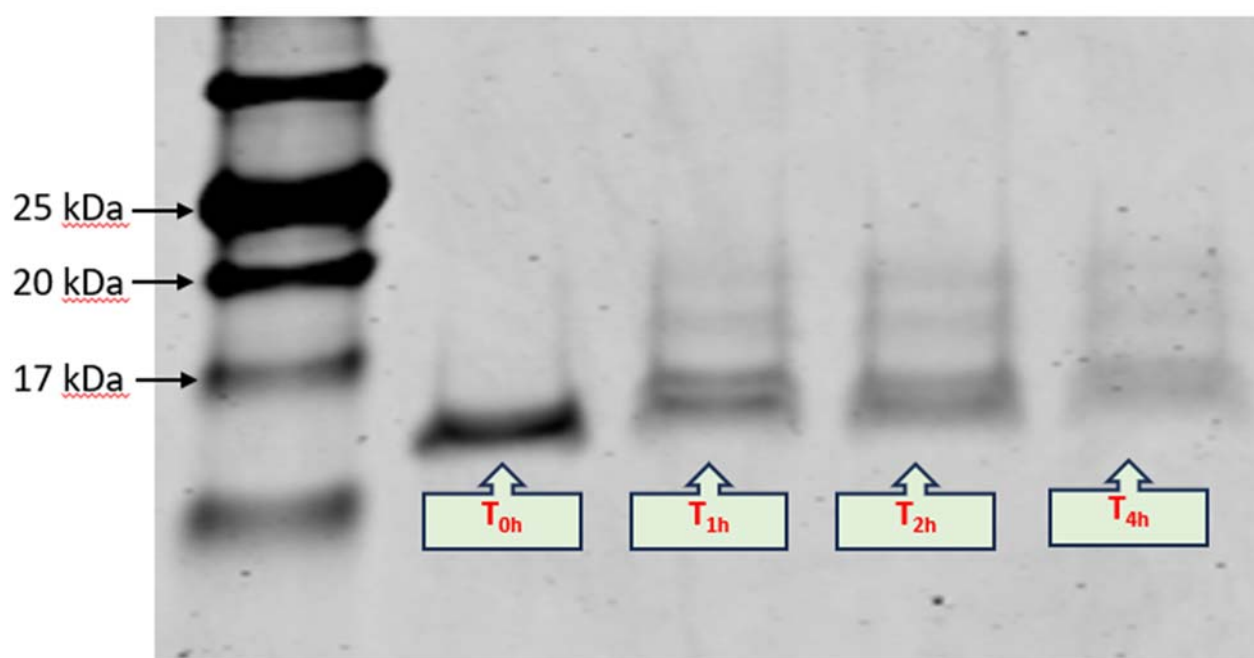
Evaluating the Time Dependent Degradation of IL-2 in HEPES Buffer

In this experiment, confirmation of the instability of IL-2 in HEPES buffer was confirmed (Figure 11). The reaction conditions were created as follows. The first buffer exchange was conducted using an Amicon 15 device and used per the protocol supplied by the manufacturer. The buffer used for this experiment was again 100 mM HEPES buffer. Once buffer exchange was complete, 6 equivalents of TLHE linker were added in DMSO under Argon

atmosphere. The final concentration inside reaction conditions was 1% DMSO. The buffer was tuned to pH 7.5 as that is more appropriate for the buffering capacity of HEPES. Lastly, this experiment was conducted at 37°C and more frequent sampling was done. The rationale behind this being that temperature only accelerates any degradation or reaction processes which occur at room temperature. The main take away from this experiment is that HEPES buffer appeared to cause IL-2 to degrade and precipitate which was visually observed after centrifuging the reaction vial at each sampling time point. The centrifugation conditions were 5 minutes at 16,000 rcf in room temperature.

Evaluating the Conjugation Reaction Using Lower Concentration of HEPES Buffer

It was theorized that the 100 mM concentration of HEPES buffer could be too high of a concentration which could be the culprit behind precipitation and degradation of IL-2 in the reaction. As a result, it was decided that only 10 mM concentration would be used to see if that would improve the poor stability of IL-2 observed in HEPES buffer (Figure 12). Unfortunately, reducing the HEPES buffer concentration did nothing to alter the IL-2 precipitation phenomenon observed. It was decided at this point that other buffer systems should also be explored as the HEPES buffer molecule itself could somehow be associated with certain IL-2 regions causing the protein to misfold and degrade.

Figure 12

Confirming instability in lower concentration of HEPES buffer
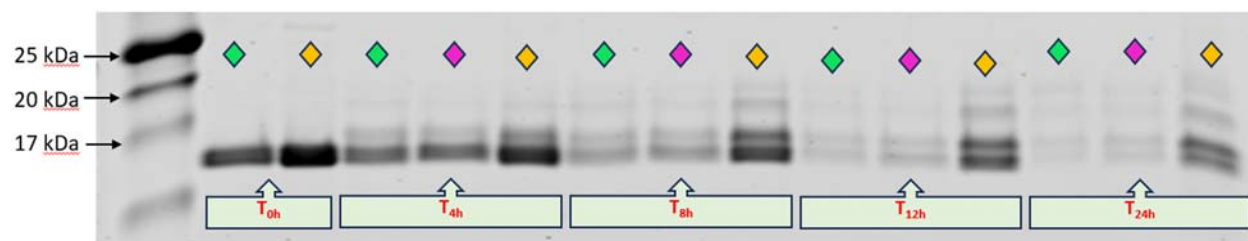
◆ **10mM HEPES**, 1% DMSO, 6 eq TLHE at T_{0h}, pH 7.5, 37°C.

◆ 10mM HEPES, **4% DMSO**, 6 eq TLHE at T_{0h}, pH 7.5, 37°C.

◆ 10mM Ammonium Acetate, 4% DMSO, 6 eq TLHE at T_{0h}, pH 6.5, RT

Evaluating the Conjugation Reaction in Tris Buffer System. This experiment was done in a very similar fashion to the 10 mM HEPES reaction study. The only difference here was that the Tris buffer system was used at a lower concentration of 10 mM. A similar phenomenon of precipitation and misfolding was observed in a time dependent manner (Figure 13). The established benchmark reaction conditions with 4% DMSO appear to remain the most optimal.

Figure 13

Evaluating the conjugation reaction in Tris Buffer
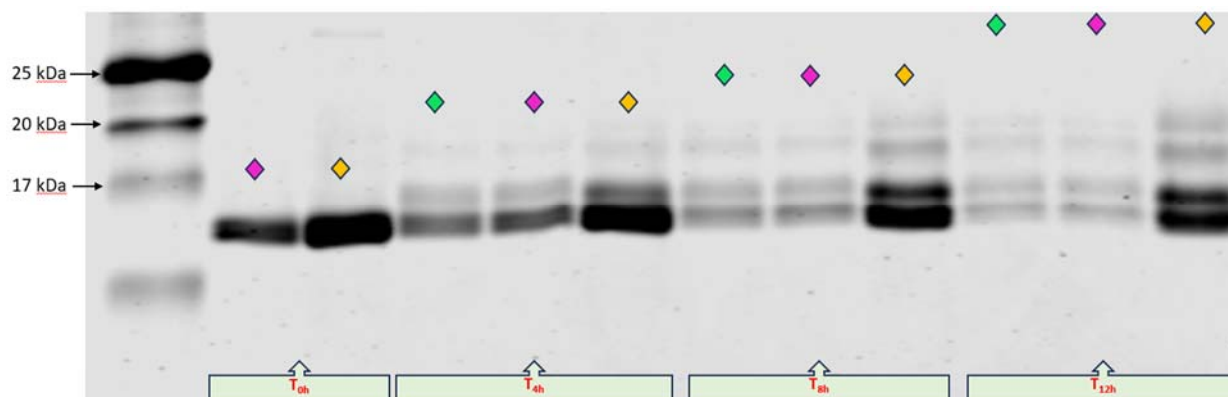
◆ **10mM Tris**, 1% DMSO, 6 eq TLHE at T_{0h}, pH 8, 37°C.

◆ **10mM Tris**, **4% DMSO**, 6 eq TLHE at T_{0h}, pH 8, 37°C.

◆ 10mM Ammonium Acetate, 4% DMSO, 6 eq TLHE at T_{0h}, pH 6.5, 37°C.

Evaluating the Conjugation Reaction in PBS Buffer System

The ability of PBS buffer to act as a superior buffer system was studied in this experiment (Figure 14). Furthermore, two different temperatures were used to fully observe if the degradation would occur faster at elevated temperatures. The methodology for this experiment was very similar to previous HEPES and Tris buffer trials where buffer exchange was done using an Amicon 15 device per the manufacturer protocol. As is evident, IL-2 exhibited precipitation which was directly correlated with longer time and higher temperature.

One major takeaway at this point which should be noted is the benchmark reaction condition which gave the best outcomes thus far. That being, 10 mM Ammonium Acetate buffer with 4 % final DMSO concentration at pH 6.5 for 24 hours at room temperature. This condition was the first condition to provide a higher percentage of TLHE-IL-2 (44%) compared with

unconjugated IL-2 (42%). Despite this, when comparing the amount of desired TLHE-IL-2

conjugate formed in comparison to starting amount of IL-2, only a 27% yield is observed.

Figure 14

Evaluating the conjugation reaction in PBS Buffer
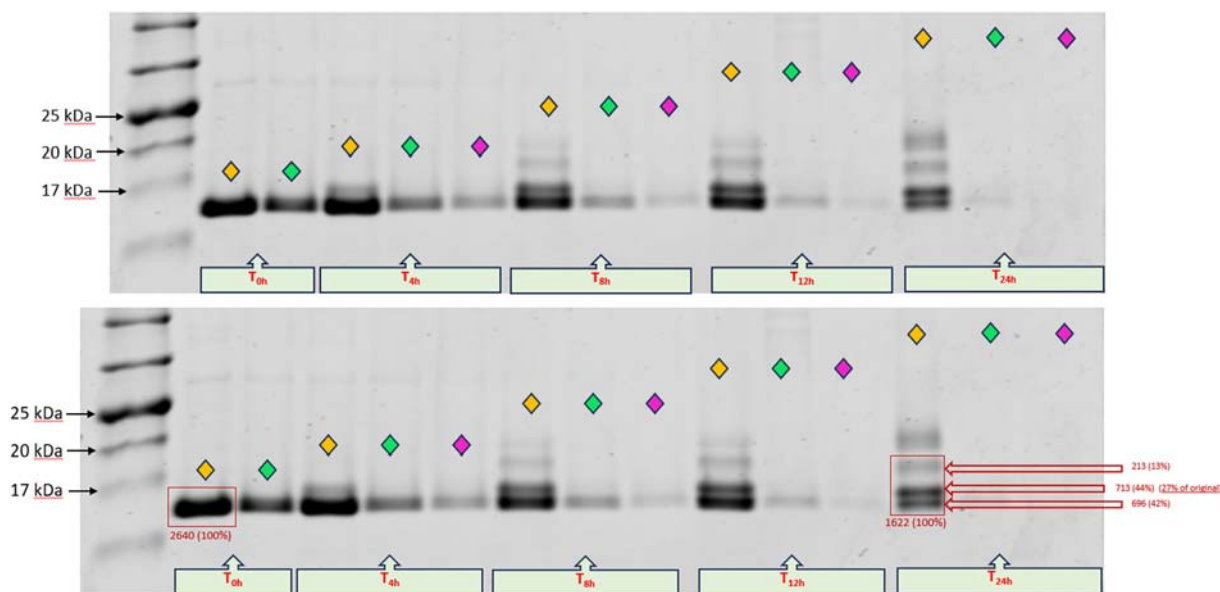
◆ 10mM Ammonium Acetate, 4% DMSO, 6 eq TLHE at T_{0h}, pH 6.5, RT.

◆ PBS buffer, 1% DMSO, 6 eq TLHE at T_{0h}, pH 7.5, RT.

◆ PBS buffer, 1% DMSO, 6 eq TLHE at T_{0h}, pH 7.5, 37°C.

Evaluating the Conjugation Reaction by Increasing pH

The thiol maleimide conjugation reaction is a click reaction which is selective for thiolate

anion nucleophiles over amine nucleophiles due to the differences in pKa. For the case of IL-2,

the main competitive nucleophile as has been described previously is the lysine side chain

amines which have a pKa of ~10. Meanwhile, the pKa of the thiol found in the side chain of

Cys-3 has a pKa of ~8. Knowing this information, it was decided to increase the reaction pH from the standard 6.5 to a pH of 7.5 to increase the formation of thiolate anion which could potentially improve conjugation outcomes. The risk which was presented by increasing the pH of the reaction, however, was that more of the amine side chains could theoretically become nucleophilic.

The result of this experiment showed that increasing the pH did not appear to improve reaction outcomes (Figure 15). Instead, the higher pH simply increased the unwanted side reactions marginally. Furthermore, it was observed that conjugated TLHE-IL-2 product was again linked via lysine side chains which caused a reduction in desired product.

Figure 15

Using higher pH to improve conjugation reaction outcomes
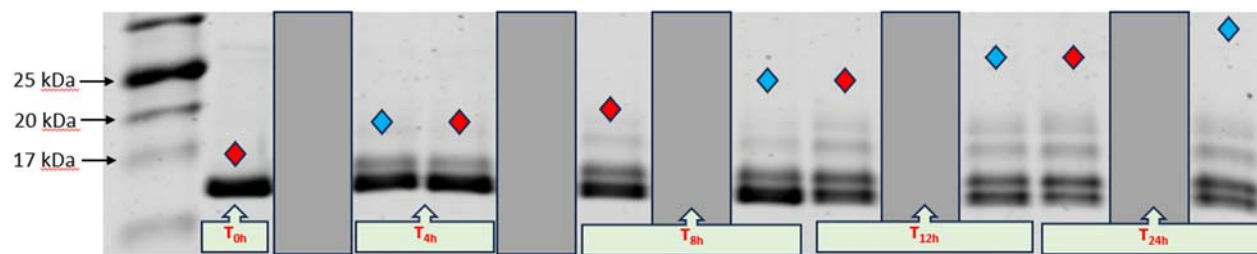
◆ 10mM Ammonium Acetate, 4% DMSO, 6 eq TLHE at T_{0h}, pH 7.5, 37°C.

◆ 10mM Ammonium Acetate, 4% DMSO, 6 eq TLHE at T_{0h}, pH 6.5, 37°C.

Reducing TLHE Equivalents by Increasing IL-2 Concentration

In this experiment, it was hypothesized that not all of the IL-2 inside the reaction was available for reaction. In other words, all the available Cys-3 thiol groups were being conjugated and remaining TLHE linkers simply reacted with the Lysine side chains. To test this hypothesis,

the same benchmark reaction condition was employed as a control group (Figure 16, green

diamond) and another group was created with the only difference being the amount of IL-2. The

yellow diamond group contained IL-2 at a concentration of approximately 2 mg/mL which is

double what the standard reaction condition used. Of note, the yellow group with higher

concentration displayed considerably more precipitation post centrifugation.

The results of this study indicated that even though the TLHE linker equivalents were

reduced, it did not seem to drastically affect any major reaction outcomes. This could suggest

that a portion of the IL-2 population present in the reaction vial did not have available Cys-3

thiol groups exposed for conjugation. One explanation for this observation could be the

formation of intermolecular disulfide bonds between the Cys-3 thiol groups.

Figure 16

Reducing TLHE equivalent ratio compared to IL-2 in the reaction

◆ 10mM Ammonium Acetate, 4% DMSO, 3 eq TLHE at T_{0h}, pH 6.5, 37°C. (double IL-2 conc. but same amount TLHE)

◆ 10mM Ammonium Acetate, 4% DMSO, 6 eq TLHE at T_{0h}, pH 6.5, 37°C.
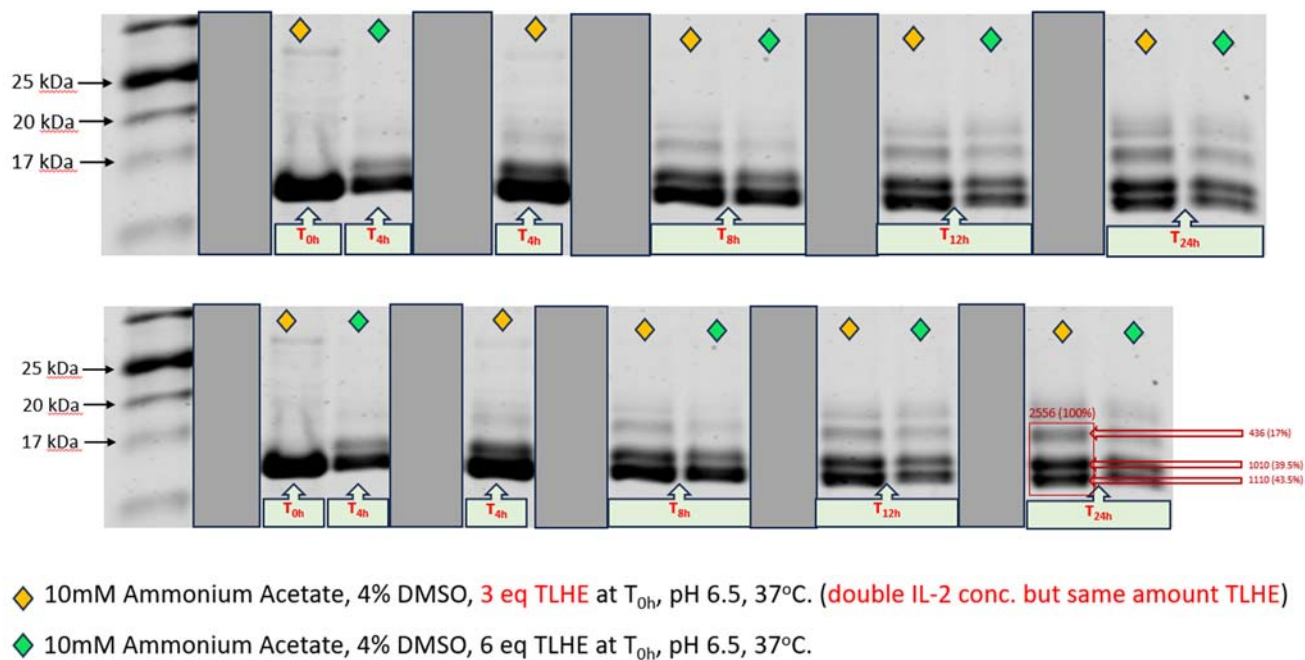
<u>Note.</u> The yellow diamonds had double the protein load compared to green diamond wells.

Evaluating the Conjugation Reaction in 4 °C

In this study, it was theorized that by reducing the temperature and slowing down the reaction rate, an enhanced selectivity for the Cys-3 thiol group could be seen. The result of this experiment however showed no appreciable benefit by conducting the reaction at 4 °C (Figure 17). More importantly, there was an appreciable loss in yield by the 72 hour timepoint when compared with the 24 hour timepoint.

Figure 17

Conjugation Reaction attempted at 4 °C
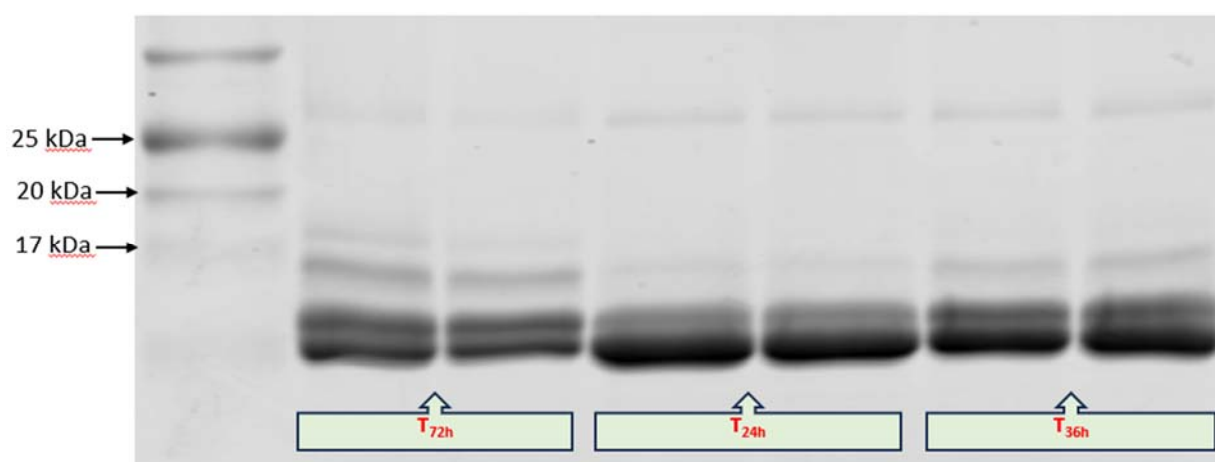
Elution Studies

Results of Mini-whole Gel Elution

In this experiment, an example prep-gel (Figure 18) was eluted using the Mini Whole Gel Eluter apparatus from BioRad. Considering the extremely poor yield seen in Figure 19, it was concluded that the majority of the eluent protein ran through the bottom of the collection wells. These collection wells were a previously known risk where if the elution electrophoresis was run for too long, then the protein could move right through the bottom. To further support this

hypothesis, the prep gel which underwent elution electrophoresis was Coomassie stained to check. As evident in Figure 20, the staining demonstrated that the majority of proteins were no longer inside the gel. It was decided that shorter run times should be explored in order to prevent protein elution past the cellophane bottom barrier of the collection wells. Unfortunately, BioRad ceased to provide product support for this device and therefore did not sell any of the expendable materials required for its use, such as the bottom cellophane and filter paper. To solve this dilemma, it was decided to purchase the alternate device which BioRad sold, named the Model 422 Electro Eluter.

Figure 18

Example of preparatory SDS PAGE gel used for Mini Whole Gel Elution. This gel was stained for visualization with use for Model 422 Electro-Eluter with Coomassie dye
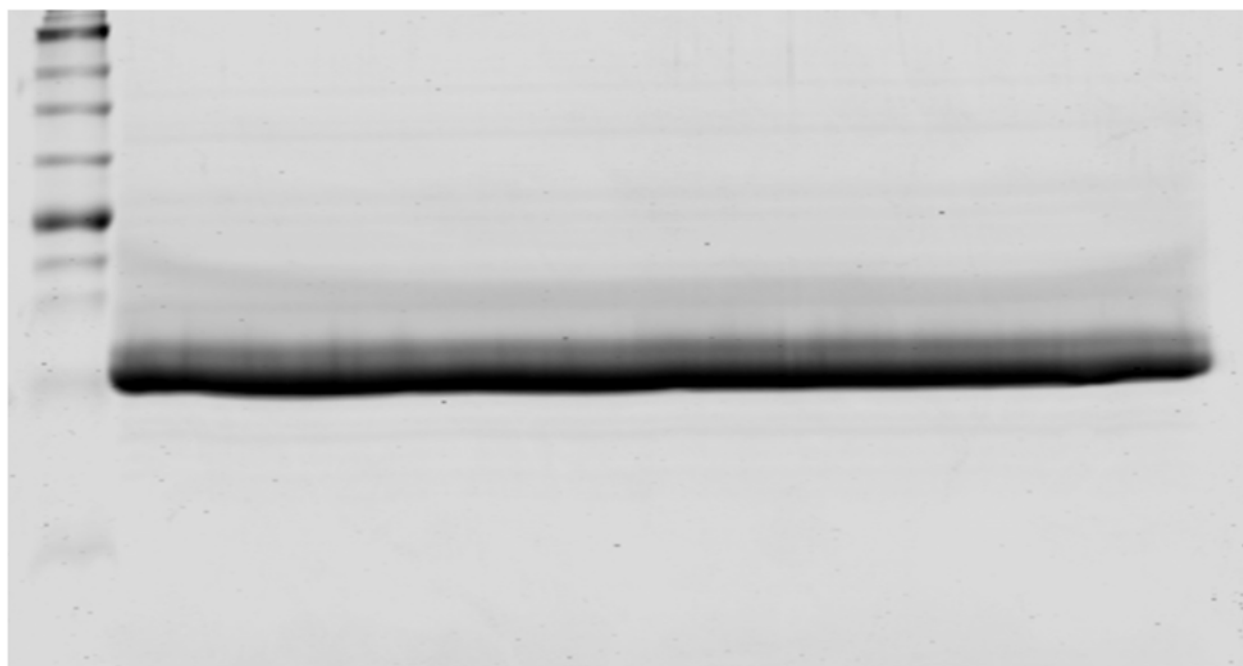
Figure 19

Result of loading elution samples from Collection-Wells# 2-14
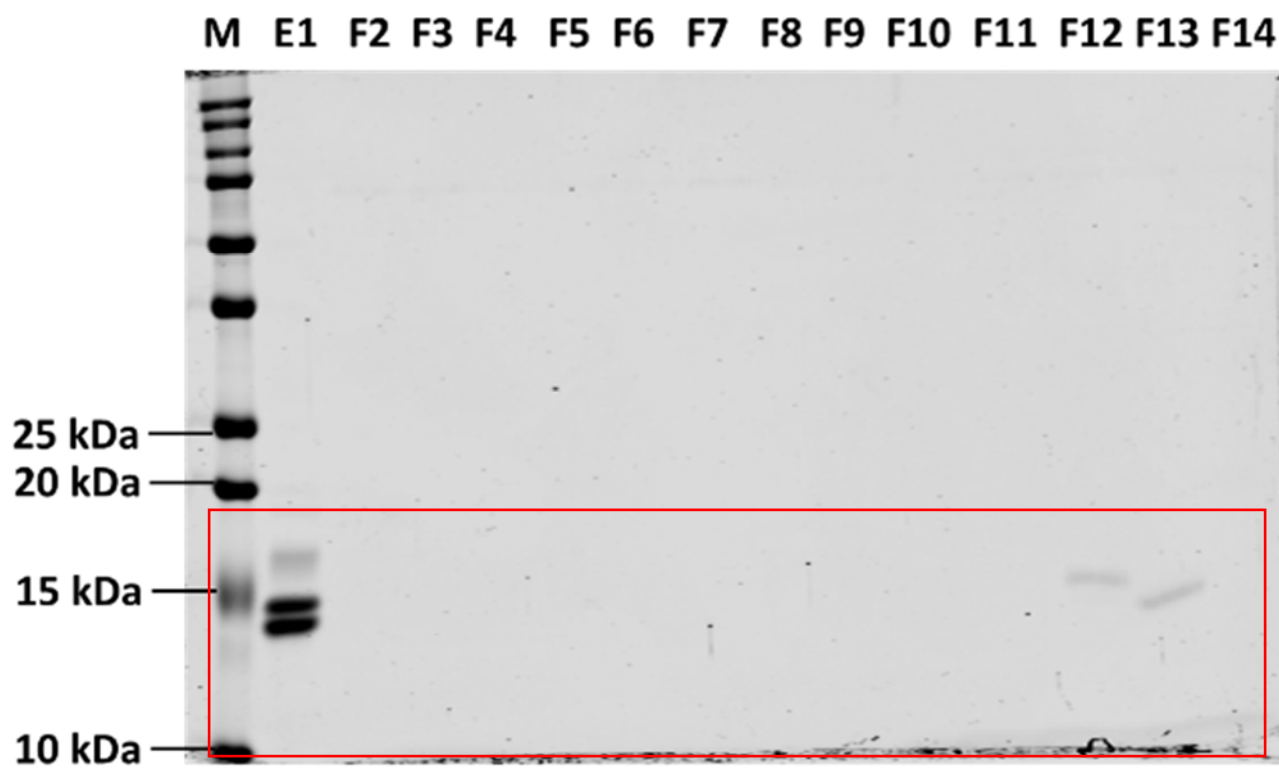
Note. Below is a zoomed in version of the contents of the red box above.

Figure 20

Coomassie staining gel post Mini-whole Gel Elution

15% one well gel stained after the elution

TLHE-rIL2

rIL2
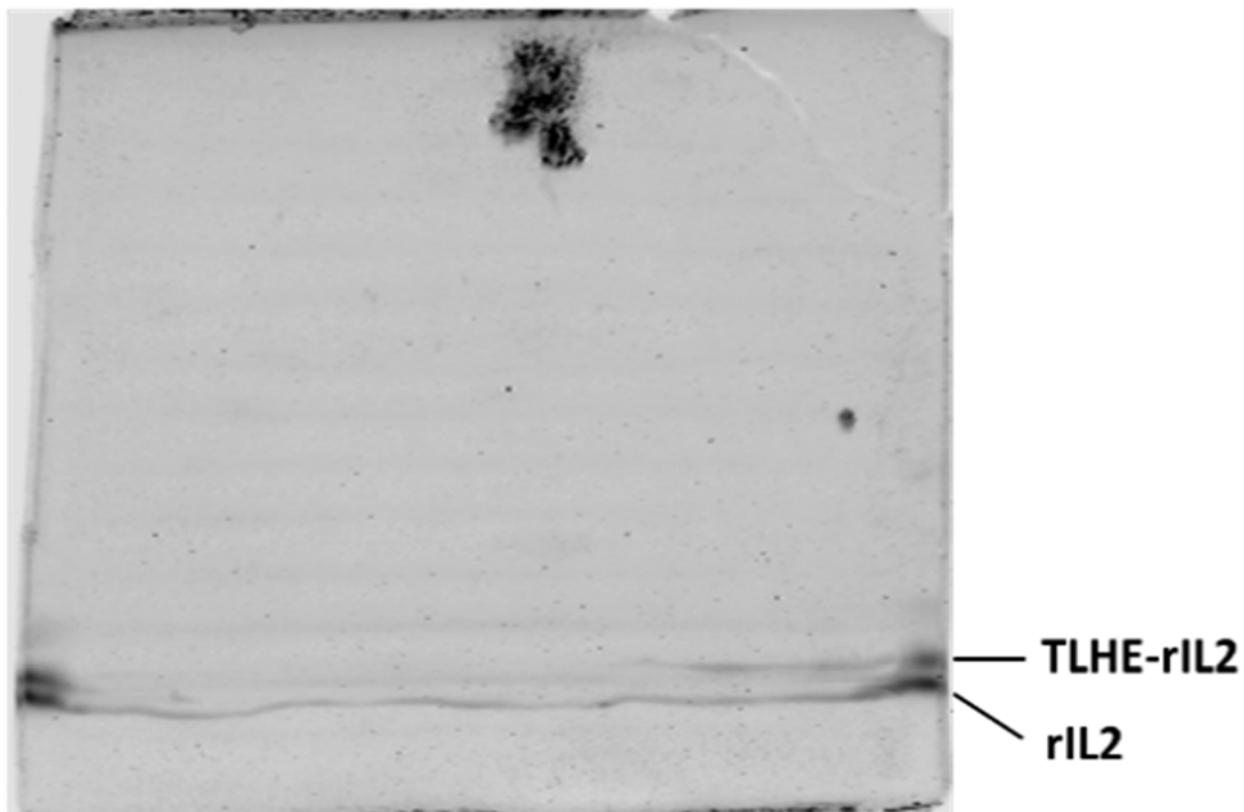
Attempts to Isolate TLHE-IL-2 Via the Model 422 Electro Eluter

       Significant precipitation was seen when the denatured IL-2 sample in 8 M Urea was slowly added into the modified redox refolding buffer containing 2 M Urea. This sample was centrifuged for 10 mins at 20 °C at 16,000 rcf. The precipitated pellet was loaded onto the gel for each both group A and B (Figure 21: two right most lanes). It was concluded from this experiment that the Urea refold approach was not viable to refold the eluent conjugate protein. The majority of the protein precipitated out and failed to refold.

It is important to explain the rationale for the methodology adopted where 6 M Guanidine HCl was first used to solubilize the inclusion body, followed by dialysis to 8 M Urea. This was because 8 M Urea exhibited distinct solubilization capabilities for IL-2 inclusion bodies in comparison to 6 M Guanidine HCl based on experiments. The focus of this stage was to investigate the mini-hypothesis on the potential of refolding the protein from its soluble state in 8 M Urea. It is important to note a distinction where there exists a difference between the capacity of a chaotrope to dissolve proteins that are initially insoluble and its capacity to sustain the solubility of a protein that has already undergone denaturation. Therefore, based on the findings from previous experiments which demonstrated the superior solubilization ability of 6 M Guanidine HCl compared to 8 M Urea for IL-2 inclusion bodies, the experimental protocol was modified to accommodate this variation in the chaotrope properties.

To clarify, the difference between the standard IL-2 harvesting method stated in Methods section 1.2.1.2 and the refolding method employed in this experiment is twofold. The first point of variance is the dialysis from 6M Guanidine/100 mM Tris, 300 mM NaCl, pH buffer to 8 M Urea/ 100 mM Tris/ 192 mM Glycine/ pH 8.3 to closely emulate the buffer used in the elution electrophoresis buffer. The second point of variance is the refolding redox buffer utilized which was modified in this study to explore the main hypothesis of the experiment. The main hypothesis being whether replacing 1.1 M Guanidine HCl in the refolding buffer with 2 M Urea would be a viable method to refold the eluted TLHE-IL-2.

SDS was not included in the 8 M Urea buffer composition because the objective of this experiment was to provide a refolding method using Urea. One argument which could be made here is that the elution electrophoresis buffer contains 0.1% SDS while the experiment did not include any SDS. The counterpoint to this idea is that the presence of 0.1% SDS, the protein

would remain in a denatured form. This assumption was drawn because even in the SDS PAGE gel electrophoresis, which was used to study the results of conjugation reactions, there was TGS buffer containing 0.1% SDS. This environment of 0.1% SDS without 8 M Urea, was enough to maintain denaturation of the protein. Furthermore, it is known that SDS binds through electrostatic attraction association with positive charges on the protein. As a result, SDS would prevent refolding, and therefore reject the premise of the entire experiment. If the approach using a Urea refold was adopted, the challenge of SDS removal would remain, necessitating the Pierce Thermofischer Detergent removal column.

Lastly, it was known that residual SDS would prevent refolding in the standard 1.1 M Guanidine HCl refolding redox buffer. This was seen in an experiment where the eluent in 8M Urea/ TGS buffer was dialyzed against 8 M Urea/ TG buffer (-SDS). Following this removal of excess unbound SDS, the sample was added into 1.1 M Guanidine refolding redox buffer. At this step, complete protein precipitation and degradation was observed.

Figure 21

Result of Urea refold study as described in the methods section 1.2.2.2.2.1
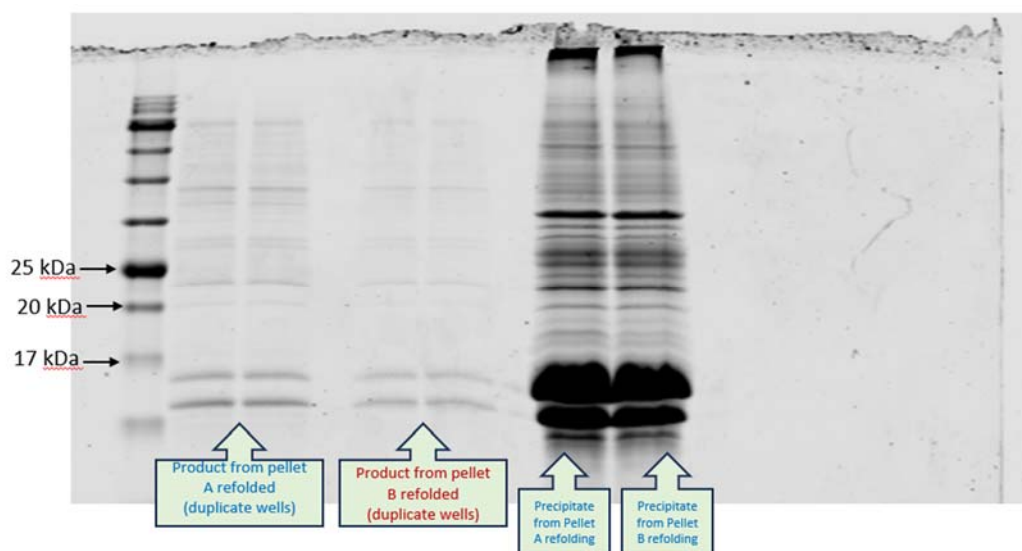
Pierce Thermofischer Detergent Removal Column and Refolding. This experiment validated the use of the Pierce ThermoFischer Detergent Removal Column to remove SDS from the eluent sample and then refold using the standard Guanidine HCl method. (Methods 1.2.1.2). Briefly, two vials of pre-aliquoted IL-2 of verified purity and concentration (SDS-PAGE and BCA assay) were dialyzed against 8M Urea/ TGS buffer. This sample was then added to the Pierce Thermofischer Detergent removal column and washed with 8M Urea/ TG buffer (same buffer but without SDS). This sample now in 8M Urea buffer without SDS was then dialyzed against the standard inclusion body solubilization buffer of 6M Guanidine HCl/ 100mM Tris/ 300mM NaCl/ pH 8. At this point, the sample underwent the same refolding protocol as in Methods 1.2.1.2. The Yellow diamond (Figure 22) signifies a sample taken before the experiment started. Green diamond was the refolded protein after elution from Cobalt-IMAC. Lastly, it is known that removal of Imidazole can cause residual amounts of protein to precipitate. Thus, the

pink diamond validated that even after removal of Imidazole, the protein was stable. This

formulation of buffer and protein was what was previously used in-vitro and in-vivo studies.

Figure 22

Result of Pierce Detergent Removal Column and Guanidine HCl refold
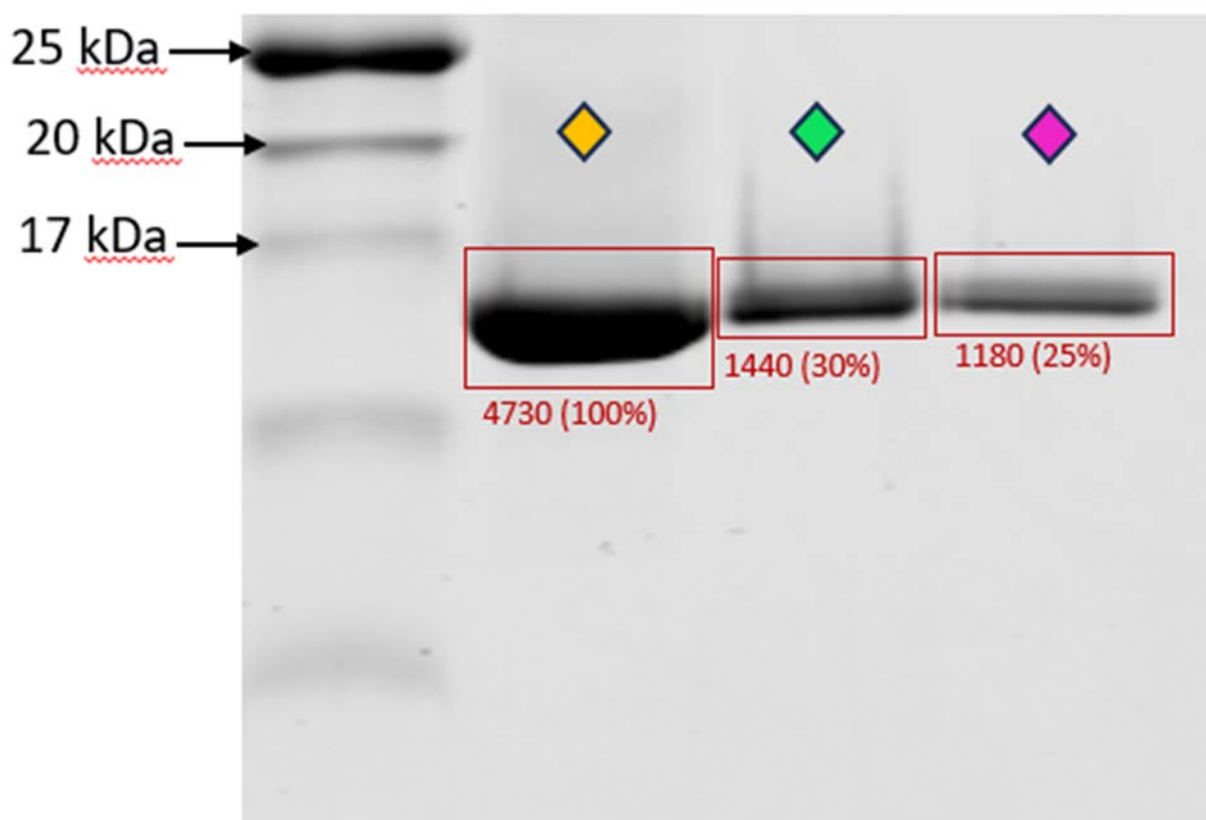
◇ Sample <u>before</u> undergoing denaturation/refold.

◆ Sample <u>after</u> undergoing denaturation/refold but still contained 0.5M Imidazole from Cobalt purification column. (10mM Ammonium Acetate, pH 6.5 + 0.5M Imidazole)

◆ Sample <u>after</u> undergoing denaturation/refold and dialyzing out Imidazole. (only 10mM Ammonium Acetate, pH 6.5)

Post Elution Sample of Isolated TLHE-IL-2 Before Refolding. This experiment was

conducted after validating each step of the Model 422 Electro Eluter approach. Each previous

experiment proved the solutions to the various aforementioned technical challenges to be valid.

The Elution conditions, removal of SDS, and refolding were each individually tested and found

viable to apply to a prep gel of the conjugation reaction. Consequently, all the optimized insights

were taken and applied to a preparatory SDS PAGE gel (example pictured in Figure 18). The

desired conjugate band of interest was excised and broken into small 1 cm x 1 cm fragments

which were then eluted. The left two yellow diamond groups are duplicate samples from the

conjugation reaction to validate the formation of desired conjugate. The pink and red diamonds

are the post elution and post SDS removal samples.

Figure 23

Post Elution Sample of isolated TLHE-IL-2 before refolding
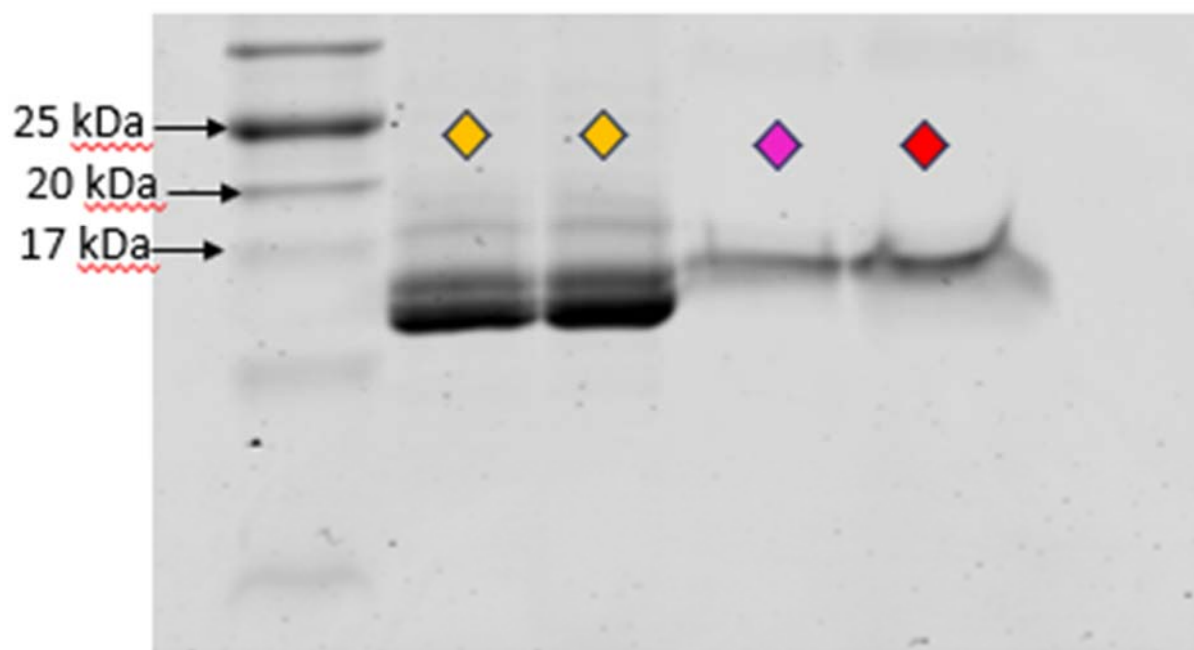
◆ Sample from prep reaction as reference. (ran in duplicate)

◆ Sample which was extracted from prep gel slice (before refolding). (15uL Load of eluent)

◆ Sample which was extracted from prep gel slice (before refolding). (30uL Load of eluent)

Post Refolding of Isolated TLHE-IL-2 Protein in 8 M Urea. This last experiment successfully isolated the conjugate TLHE-IL-2 from all other components of the conjugation reaction, albeit with an unfavorable yield. As can be seen in the green diamond groups, efficiency comparing cumulative IL-2 and conjugates in the reaction and what remained after refolding, was around 2%.

Figure 24

Post Refolding of isolated TLHE-IL-2 protein depicted in Figure 23

25 kDa →
20 kDa →
17 kDa →

4670   4850

(Avg= 4760)

113 (~2.3%)   84 (~1.8%)
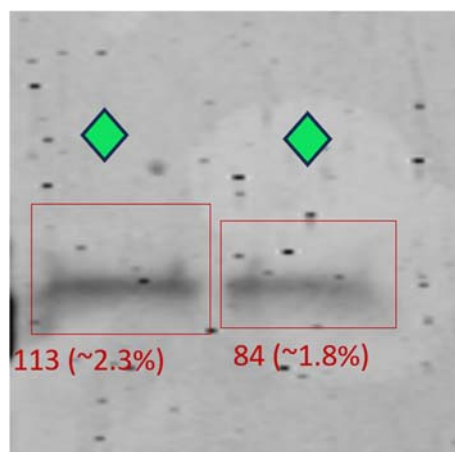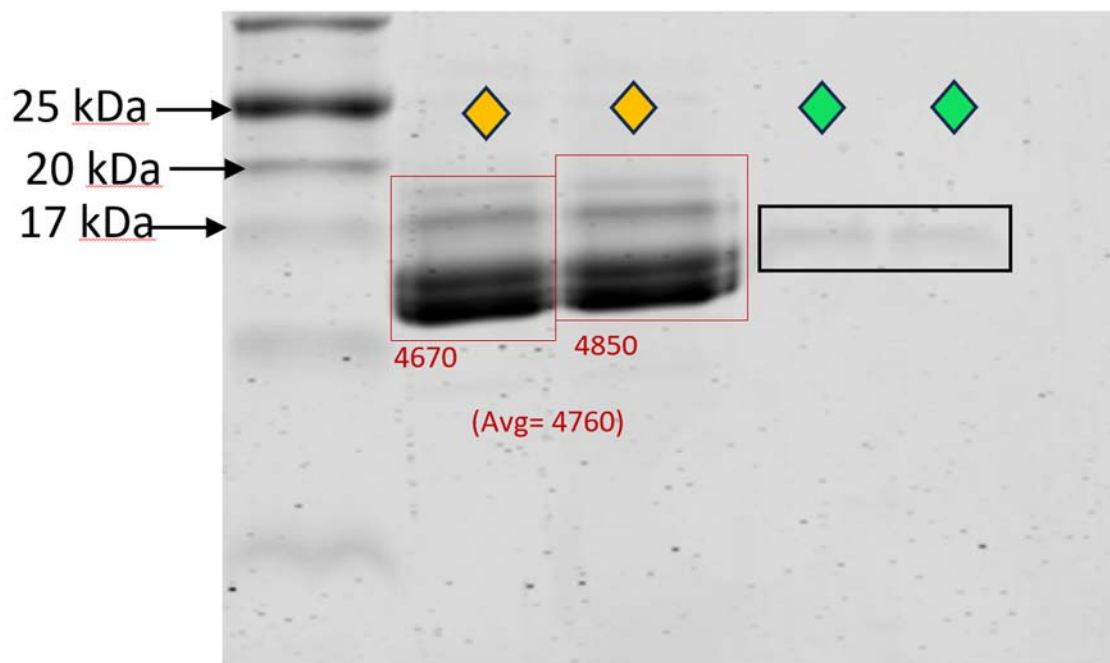
◇ Sample from prep reaction as reference. (ran in duplicate)

◇ Refolded eluent. (ran in duplicate). (still had 0.5M Imidazole; did not dialyze).

Discussion

From the conjugation reactions, we learned that increasing the DMSO concentration in the reaction mixture from 1% to 4% resulted in better solubility of the TLHE linker, which improved reaction outcomes. It is known that the IL-2 present in buffer is soluble and stable in the 10 mM Ammonium Acetate, pH 6.5 buffer. Therefore, it can be postulated that the benefit in conjugation is due to enhanced TLHE linker solubilization. Furthermore, it is known based on the linker structure that its aqueous solubility even in 1% DMSO could be limited.

One puzzling observation seen was the instability of IL-2 in other aqueous buffers, notably HEPES, Tris, and PBS. These buffers could cause conformational changes in IL-2 leading to its misfolding and subsequent precipitation.

Regarding the elution studies, despite their success, the cumulative yield starting from aliquoted IL-2 to post refolding after gel excision and elution was approximately 1.2%. This number is calculated by finding approximately 60% recovery of cumulative protein in <u>Figure 14</u>. When the original IL-2 intensity is used as original amount (2640 units) and compared with the cumulative protein bands seen after 24 hours of reaction (1622 units), the conjugation recovery can be found. Furthermore, efficiency when comparing cumulative IL-2 and IL-2 conjugates in the reaction (avg. 4760 units) versus what remained after refolding (~100 units), was around 2%. (<u>Figure 24</u>). As a result, the cumulative yield was around 1% starting from the expressed and purified IL-2. Considering the commonly required dosing for in vivo efficacy studied in mice, it was no longer practical to use this approach to generate pure TLHE-IL-2 in sufficient amounts to conduct viable experiments.

CHAPTER 2: ENHANCING THE EFFICACY OF PEPTIDES THAT INHIBIT COVID 19
VIRAL ENTRY

Abstract

What would happen to a viral infection if suddenly there were a billion fake receptors for every real target receptor. A version of this question is what led to the development of a novel HIV therapy at Duke University around 1996. Fast forward more than 30 years, man still lacks the proper tools to combat viral infections. One can argue that the Achilles' heel of viral infections is their need to bind a specific receptor. This protein-protein interaction between viral proteins and human receptors is arguably the fundamental point behind all viral infections. Recently, the COVID-19 pandemic again challenged man to develop new weapons at a revolutionary pace in order to save lives. During this time, the Pentelute lab at Massachusetts Institute of Technology reported a humanized version of the peptide sequence thought to represent the binding face of the human ACE2 receptor[41]. The 23 amino acid sequence was derived from the α1 helix of ACE2 peptidase domain and referred to as, spike-binding peptide 1 (SBP1). It was this sequence which was postulated to be responsible for binding the receptor binding domain of the notorious COVID-19 spike protein. However, a major limitation of peptide is their short in vivo half-life (through serum proteases and renal filtration). Therefore, the main aim of our proposed research was to employ the TLHE approach to extend the in vivo half-life of the SBP1 peptide. This would allow the creation a COVID-19 entry inhibitor that could help combat the COVID-19 pandemic.

Introduction

The COVID-19 pandemic has resulted in a significant global impact, causing millions of fatalities owing to its severe respiratory manifestations. When this work was undertaken, in

August of 2020, a significant challenge persisted as medical teams lacked access to dependable

medication to effectively combat this formidable threat. Common manifestations of COVID-19

encompass respiratory symptoms such as cough, fever, and dyspnea, among others. The elderly,

those with obesity, smokers, and individuals with hypertension are patient categories that exhibit

heightened vulnerability to this particular condition[23]. Finally, the airborne transmission rate of

this virus in close proximity to one another has rendered it notably problematic. Thus far, several

endeavors have been made to combat this viral infection, yielding varied outcomes. These efforts

encompass the utilization of antiviral agents like remdesivir and hydroxychloroquine, as well as

those of vaccines and investigational antibodies. Remdesivir, a small molecule antiviral agent,

has demonstrated efficacy in expediting patient recovery; however, its effectiveness appears to be

diminished in cases with severe COVID-19. Furthermore, uncertainties persist regarding the

potential of remdesivir to mitigate the mortality risk associated with COVID-19.

One primary prospective strategy for halting the progression of this disease is the

prevention of viral entrance into human cells. This approach has resemblance to the widely

recognized HIV entry inhibitors, such as Enfuvirtide, which are employed in combination

therapy for managing HIV-1 infection. Viral entry inhibitors have several advantages, such as the

potential to decrease the average length of sickness, prevent the onset of infection, and mitigate

the intensity of disease symptoms. In order to achieve this objective, peptides are favored over

small compounds due to their capacity to disrupt extensive binding surfaces and engage with

various sites of protein-protein interactions between the virus and human cells.

The initiation of the COVID-19 virus entry into human cells occurs through the contact

between the receptor binding domain (RBD) of its viral spike protein and the angiotensin-

converting enzyme 2 (ACE2) transmembrane receptor present on the surface of human cells. The

potential therapeutic intervention of inhibiting the protein-protein interaction between the RBD

and ACE2 through the use of target-specific medicines holds promise for potentially saving lives.

Moreover, the utilization of a secure chemical that inhibits viral entrance possesses several

preventive implications in mitigating the continued dissemination of this worldwide public

health emergency.

What Are Entry Inhibitors?

Entry inhibitors are compounds which act by preventing the penetration of viruses into

host cells. This class of compounds also incorporates molecules known as fusion inhibitors

which act in a similar manner wherein, they inhibit the occurrence of conformational changes

necessary in the viral envelope for subsequent viral entry to occur[42]. This approach is seen

illustrated in Figure 25 with its various flavors of action.

Figure 25

Summary of entry inhibitor approaches compared visually[24]
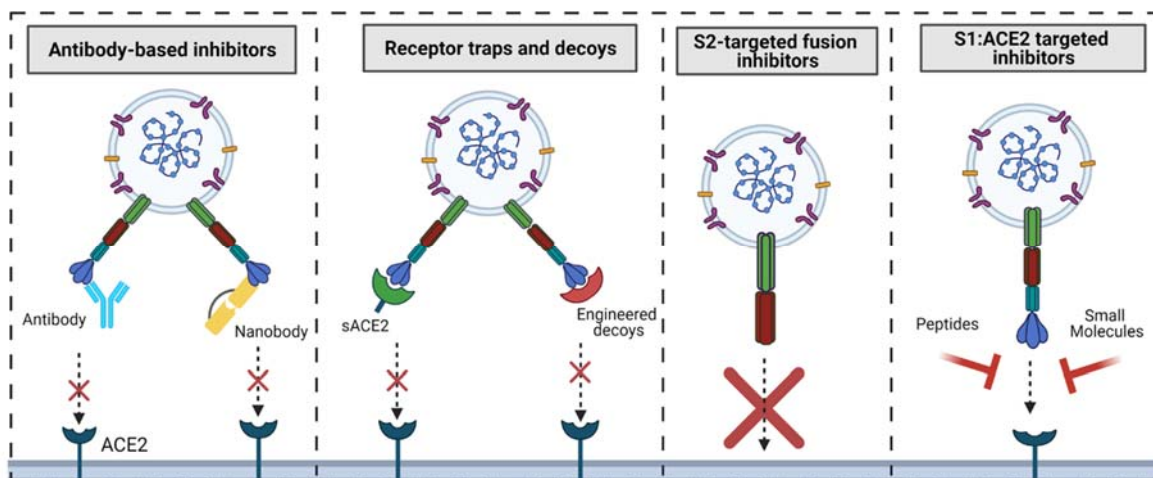
Chapter Objective and Hypothesis

Hypothesis of the study: conjugation of TLHE with SBP1 will extend the circulation half-life of the SBP1 peptide without compromising binding affinity to SARS-CoV-2-RBD.

Outline of Proposed Studies

    a. Synthesize the TLHE-SBP1 conjugate.

    b. Evaluate binding of TLHE-SBP1 conjugate to TTR and SARS-CoV-2-RBD.

    c. In vitro and in vivo Pharmacokinetic evaluations in rats.

    d. Evaluate live viral entry inhibition via an in vitro study.

Methods

Synthesis of SBP1 and TLHE-SBP1

Synthesis of SBP1 (sequence found in Scheme 1 and Scheme 2) was done using Rink-Amide MBHA resin preloaded with Fmoc-Ser(tBu) (resin loading: 0.51 mMol/g). Automated peptide synthesis was utilized using DIC /HOAt activation. Coupling was done over reaction times ranging from 90-120 mins at 80 ºC. Fmoc deprotection was conducted using 20% (v/v) Piperidine in DMF. Additionally, select coupling reactions in the sequence were modified to optimize purity and yield (4-Pentynoic acid, E_2, F_8, F_{12}, H_{14}, F_{20}, Y_{21}). This modification was termed "double-coupling" because it involved a repeated coupling reaction step with the same amino acid without Fmoc-deprotection. The concept behind this step was to solve a problem of poor yield and purity. It was postulated that certain residues were not being coupled onto the growing peptide chain due to sterically bulky groups in their side chains. During "double-coupling", a wash step replaces what normally would be a Fmoc deprotection step. Following this wash, a second reaction aimed at coupling the same amino acid would occur. The rationale here being that since Fmoc was not removed, unwanted doubling of the amino acid in series

would not transpire. Simply put, the coupling reactions were modified in the sense that they were actually two coupling reactions without including the Fmoc deprotection step in between.

In the synthesis of TLHE-SBP1, an added step existed wherein 4-pentynoic acid (CAS# 6089-09-4) was coupled using the same conditions as previous amino acids. This coupling placed 4-pentynoic acid as moiety located at the N-terminus before coupling through click chemistry. Lastly, click chemistry was done by reacting 4-pentynoic-SBP1 (22 mg, 7.63 µMol, 1 equivalents) with the TLHE linker (6.3, 9.74 µMol, 1.25 equivalents). Catalysts and cofactors included $CuSO_4$ pentahydrate (0.48 mg, 1.92 µmol, 0.25 equiv), and sodium ascorbate (3 mg, 15.14 µmol, 2 equiv) in a mixture of H_2O/THF (1:3) (2.4 mL).

After completion of synthesis, resin was transferred from the automated synthesis vessel into a separate reaction vessel. Here, the solvent was flushed with air and a small sample was taken for Kaiser test of the SBP1; Kaiser test was not applicable for the Pentynoic acid conjugated peptide. Next, approximately 5 mL of reagent B cleavage solution (88% TFA, 2% TIPS, 5% H_2O, 5% phenol) was added to the resin. The cleavage solution resin suspension was shaken at room temperature for 5 hours. The reaction mixture was collected in approximately 40 mL ice cold diethyl ether and the precipitate was collected by centrifugation. The precipitate was again mixed with another 40 mL diethyl ether and washed three times in the same manner. Finally, the precipitate was left to dry overnight to remove any trace diethyl ether in air.

In the case of conjugation of TLHE to 4-pentynoic-SBP1, procedure for executing the click reaction was as follows. Corresponding amounts of 4-pentynoic-SBP1 and TLHE linker were transferred into a 20 mL borosilicate glass vial and pumped under reduced vacuum pressure for four hours until exhaustively dry. Meanwhile, corresponding amounts of powdered copper sulfate-pentahydrate and sodium ascorbate were added into a 1.5 mL Eppendorf (EP) tube. This

EP tube was then flushed with argon for 10 seconds in a gentle manner with argon gas directed to hit vial walls so as to not disturb the precisely weighed content at the bottom of the vial. The reaction was then executed by adding 1,800 µL of THF into the 20 mL vial and purging with argon. Next, 600 µL of de-ionized water was added to the argon flushed EP tube. Hastily tube was again flushed with argon gas for 2-3 seconds, and rapidly vortexed for 3 seconds. Following this, the full contents of the EP vial were transferred into the 20 mL vial containing 4-pentynoic-SBP1 and TLHE already dissolved in THF with a magnetic stir bar and flushed with argon. This mixture was again thoroughly argon flushed for 10 seconds, sealed with Parafilm, and vortexed. Subsequently, the reaction mixture was vortexed and kept stirring at room temperature overnight for approximately 16 hours.

Post overnight incubation of the click conjugation between 4-pentynoic SBP1 and TLHE, the reaction was then dried under reduced pressure. Next, the material was redissolved in a solution of 4:1 ratio of buffer A (95% H_2O, 5%ACN, 0.1% TFA) and Buffer B (5% H_2O, 95% ACN, 0.1% TFA) and was then purified by HPLC. Using Waters^{TM} XBridge Prep C18 column (10X250mm, 5 µm) (Part No. 186003256). A similar procedure was used to purify SBP1, without the click reaction steps. The gradient was a linear increase from 0% to 50% Buffer B at 23 mins followed by isocratic of 50% buffer B until 25 mins and then linearly increased to 75% buffer B at 30 mins, and finally back to 0% B at 34 mins with isocratic 100% A until 36 mins. For TLHE-SBP1, elution occurred at 45/55 H_2O/ACN (v/v) with 0.1% TFA, and at 50/50 H_2O/ACN (v/v) for SBP1.The purity of collections were confirmed by analytical HPLC (purity > 95%). Conjugation of TLHE to 4-Pentynoic SBP1 yielded 13.2mg (~50% yield). The synthesis of SBP1 and TLHE-SPB1 was in collaboration with Dr. Dengpan Liang (a previous member of the Alhamadsheh lab)

Scheme 1

Synthesis Scheme of TLHE linker and amino acid sequence

Scheme 1 (continued)

WB33
Chemical Formula: $C_{11}H_{22}N_4O_4$
Molecular Weight: 274.32

1,6-dibromohexane
Chemical Formula: $C_6H_{12}Br_2$
Molecular Weight: 243.97

DMF, NaH
RT, 3hr

WB34
Chemical Formula: $C_{17}H_{33}BrN_4O_4$
Molecular Weight: 437.38

WB27
Chemical Formula: $C_8H_{14}O_3$
Molecular Weight: 158.20

KI
K2CO3
DMF
60°C, 40hr

Acetyl Acetone
Chemical Formula: $C_5H_8O_2$
Molecular Weight: 100.12

Dibromo propane
Chemical Formula: $C_3H_6Br_2$
Molecular Weight: 201.89

Methyl 3, 5 dihydroxybenzoate
Chemical Formula: $C_8H_8O_4$
Molecular Weight: 168.15

Hydrazine Hydrate/ C. HCL
Ethanol
75°C/3hr

K2CO3
DMF
ON

WB28
Chemical Formula: $C_8H_{14}N_2O$
Molecular Weight: 154.21

PBr3
1,2 dicholorethane
75°C

WB29
Chemical Formula: $C_8H_{13}BrN_2$
Molecular Weight: 217.11

K_2CO_3/ KI
DMF
ON/50°C

WB35
Chemical Formula: $C_{25}H_{40}N_4O_8$
Molecular Weight: 524.62

WB38
Chemical Formula: $C_{32}H_{50}N_6O_8$
Molecular Weight: 646.79

NaOH
THF/H2O
50°C
ON

WB36
Chemical Formula: $C_{33}H_{52}N_6O_8$
Molecular Weight: 660.81

25% TFA in DCM

TLHE Linker
Chemical Formula: $C_{27}H_{42}N_6O_6$
Molecular Weight: 546.67

Evaluating Stability of SBP1 and TLHE-SBP1 In Human and Rat Plasma

Test compounds were incubated in 1 ml of human serum at 37 °C and samples were assayed at 0,1, 2, 4, 8 and 24 hours time intervals. Samples will be processed by adding 200 μL of solvent B (95 % methanol and 0.1 % TFA in water) followed by centrifuging at 16,000 x g for 5 mins and analyzing the supernatant using the previously described validated HPLC method.

Binding Evaluations of TLHE-SBP1 and SBP1 With TTR and a Fragment of the SARS-CoV-2 Spike Protein

Evaluating Binding of TLHE-SBP1 to TTR

The evaluation was done by examining the capacity of compounds to compete with the binding of a fluorescence probe (FPE probe) to transthyretin (TTR) in human blood. The FPE probe is a thioester TTR ligand that is not fluorescent by itself, however, upon binding to the T4 binding site of TTR, it covalently modifies lysine 15 (K15), creating a fluorescent conjugate. Ligands that bind to the T4 site of TTR will decrease FPE probe binding as observed by lower fluorescence. An aliquot of 98 μL of pooled human serum (prepared from human male AB plasma, Sigma; catalogue no. H4522; TTR concentration 5 μM); was mixed with 1 μL of test compounds [all compounds were prepared as 10 mM stock solutions in DMSO and diluted accordingly with DMSO (final concentrations in human serum were 10 μM and 20 μM) and 1 μL of FPE probe (0.36 mM stock solution in DMSO; final concentration 3.6 μM).The change in fluorescence (λex = 328 nm and λem = 384 nm) were monitored using a microplate spectrophotometer reader (SpectraMax M5) for 6 hour at room temperature.

Evaluating Binding of TLHE-SBP1 to Fragment of SARS-CoV-2 Spike Protein via Biolayer Interferometry (BLI)

Evaluation of TLHE-SBP1 binding to the COVID spike protein was done by using a commercially available His-tagged fragment of the spike protein receptor binding domain

(residues 319-541). (ThermoFischer Scientific Cat#: RP-87678). This product was then immobilized onto an Octet® Ni-NTA (NTA) Biosensor (ForteBio Cat# 18-5101) and used for testing. Various compounds were then tested on the Biosensor including a soluble ACE2-Fc protein as positive control (InvivoGen Cat# fc-hace2), SBP1, and TLHE-SBP1. The BLI assay was performed at the University of California, Davis (contract research).

Pharmacokinetic Evaluation of SBP1 and TLHE-SBP1 in Male Sprague-Dawley Rats

To validate the half-life extension effects, a pharmacokinetics study was conducted in vivo. Sprague–Dawley male rats were used for this study. An extension catheter was attached to the indwelling jugular vein cannula to facilitate remote sampling. The animals were randomly divided into two groups ($N = 4$): control group and treatment group. Simultaneously, the control group will be pretreated with vehicle (sterile water) followed by a single combined intravenous dose of molar equivalent of all test compounds as described above. Blood samples were collected from each rat, via jugular vein cannula at each time point (at 0.033, 0.25, 0.5, 1, 2, 4, 8, 12 and 24 hours) postdosing and the volume will be replaced with normal saline. The plasma samples were prepared by centrifugation, precipitated with 2X solvent B (95:5, methanol-water, 0.1 % TFA), then analyzed immediately by HPLC and also confirmed by LC-MS/MS.

LC-MS/MS Method to quantitate plasma concentrations of SBP1 and TLHE-SBP1

The calibration curves used to quantitate SBP1 and TLHE-SBP1 can be found in Figure 35. The identities of SBP1 and TLHE-SBP1 were found using Q1/Q3 transition masses. The transition mass for SBP1 was 935.3/136.2 (Q1/Q3), and for TLHE-SBP1 was 852.6/136.6. The internal standard reference used was AG10 (293.2/275.2). A Waters™ XBridge C18 column with L1 packing (4.6 X 150 mm, 5μm) was used for chromatography. The method involved a mobile phase consisting of Buffer A: 95% H_2O, 5% Methanol, and 0.1% Formic Acid; Buffer B: 95%

Methanol, 5% H_2O, and 0.1% Formic Acid. The gradient involved building up to 100% buffer B within the first 5 minutes, followed by 6 minutes of isocratic at 100% buffer B, then switching to 100% buffer A in 1 minute, followed by 1 minute of 100% buffer A. The retention times were as follows: AG10 (8.7 minutes), SBP1 (8.1 minutes), and TLHE-SBP1 (8.6 minutes). Total run time of 13 minutes.

Live Reporter Virus Assay

A Nanoluciferase reporter live virus assay method was utilized by Dr. Jin Jing at Vitalant to evaluate the inhibitory effects of SBP1 and TLHE-SBP1. Etesevimab and Casirivimab, commercially available controls, were used to validate the procedure.

Results and Discussion

Serum Stability

Evaluating stability of SBP1 and TLHE-SBP1 in both human and rat plasma showed two benefits afforded through conjugation of TLHE to SBP1. Without any TTR interactions, SBP1 showed increased susceptibility to enzymatic metabolism via serum proteases. This difference can be clearly seen in Figures 26-28 where TLHE-SBP1 is able to exhibit greater stability relative to SBP1. It is important to note that this claim of TTR protecting against proteolysis needs further experiments to be fully validated. This is because the mere conjugation of TLHE at the N-terminus could sterically slow down proteolysis by acting as a block into enzymatic active sites. However, the objective of this evaluation was to validate the relative stability of both SBP1 as well as TLHE-SBP1 in plasma. Although, proteolytic stability was a welcomed characteristic conferred upon TLHE-SBP1, TLHE conjugation is mainly intended to protect against renal filtration.

Figure 26

Stability of SBP1 in Rat and Human Plasma monitored via HPLC
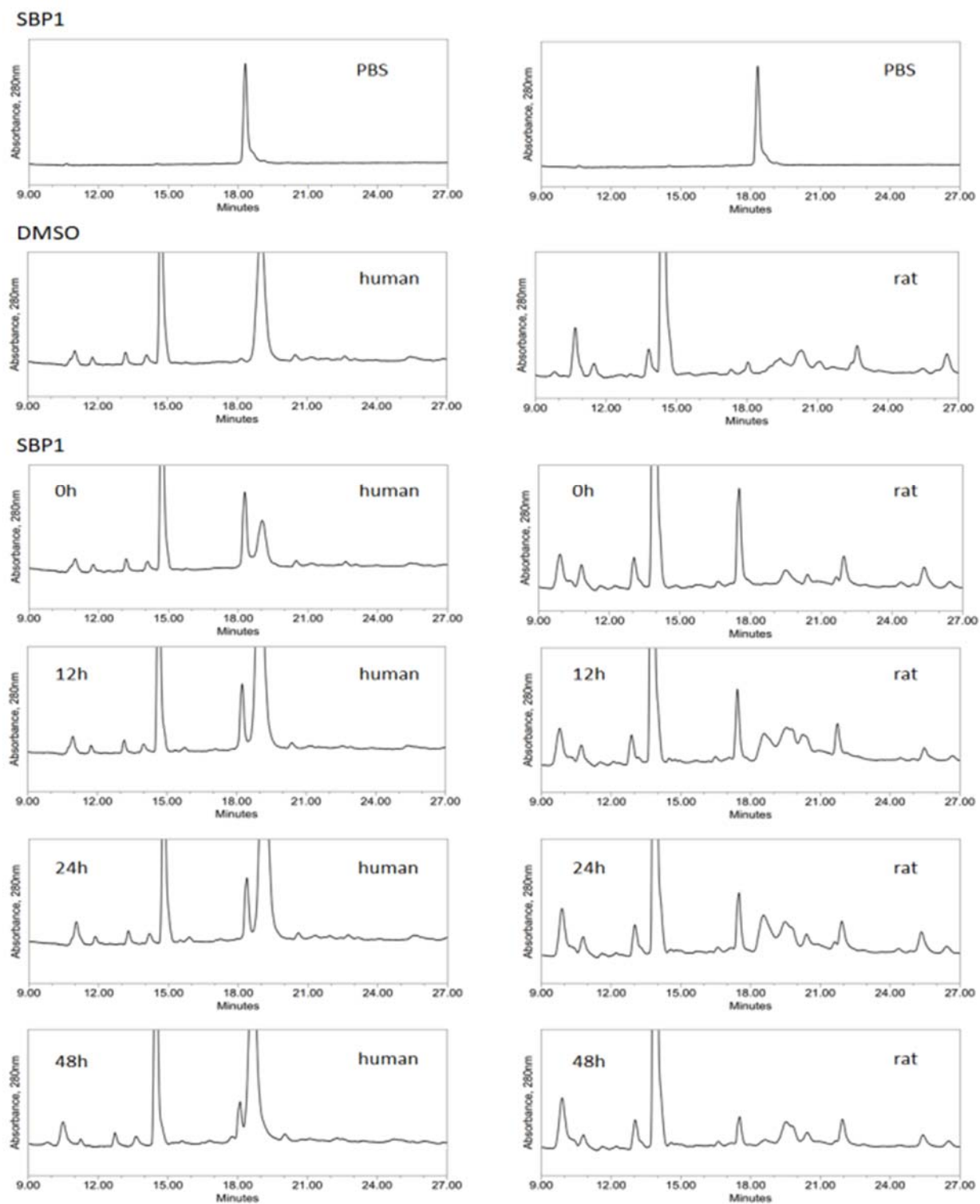
Figure 27

Stability of TLHE-SBP1 in Rat and Human Plasma monitored via HPLC
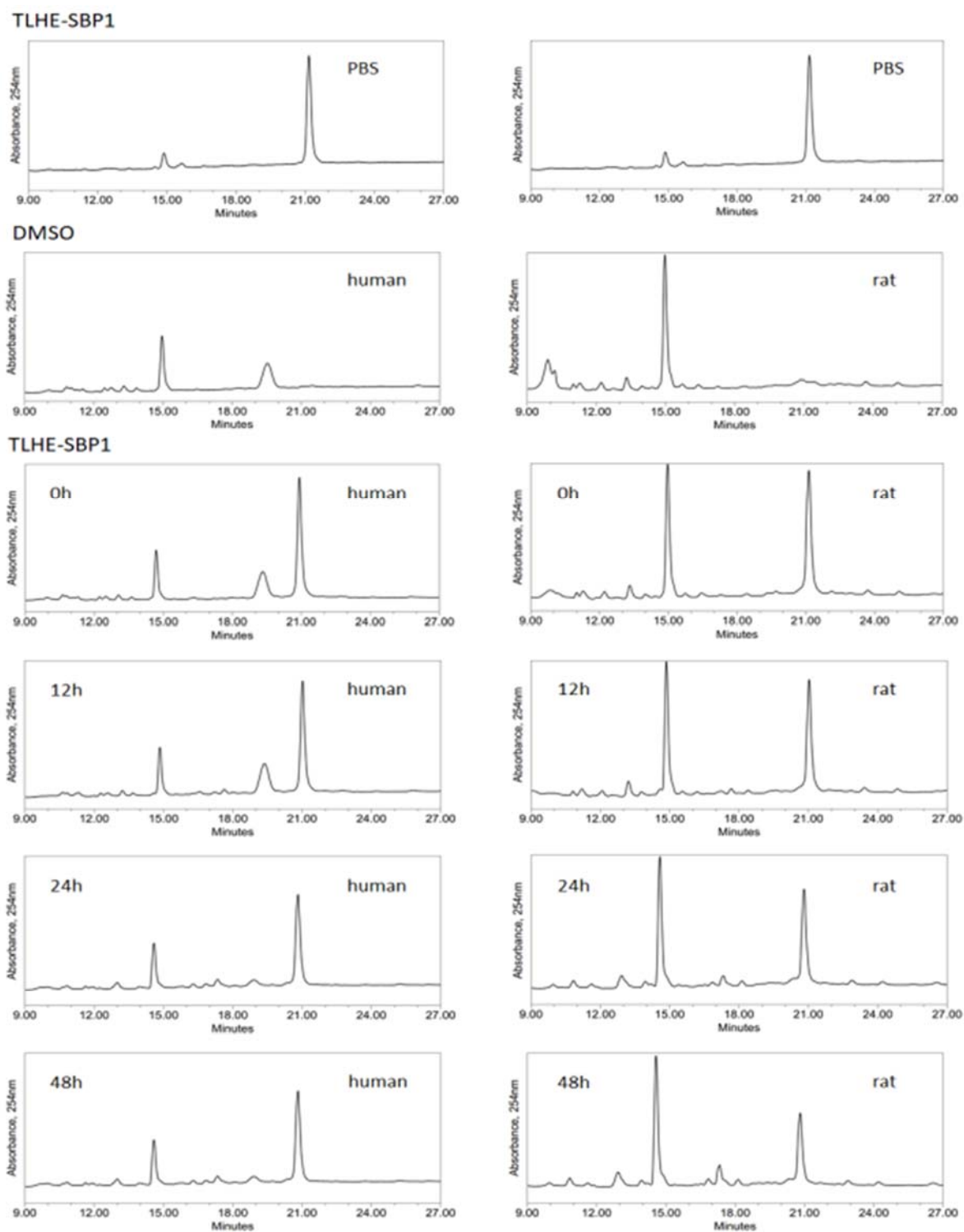
Figure 28

Graphical representations of data presented in Figures 26 and 27
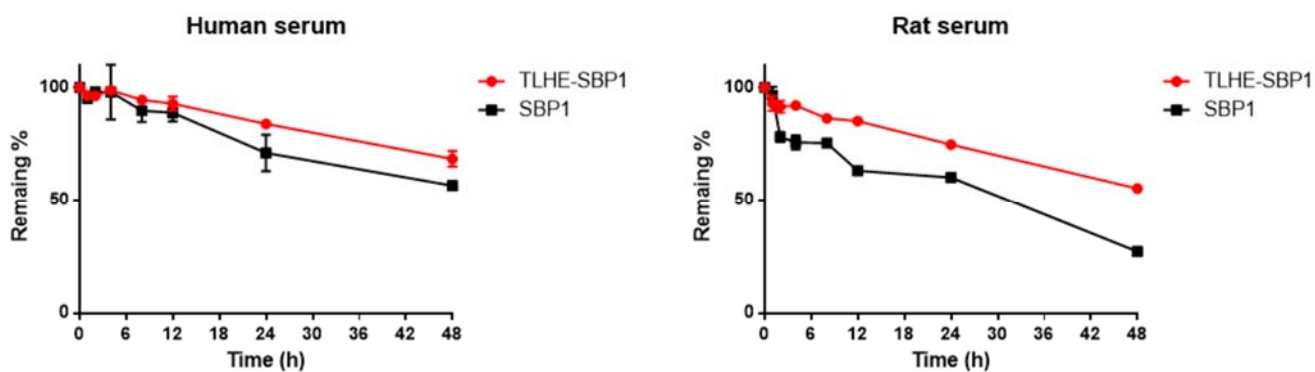
Evaluating Binding Characteristics of SBP1 and TLHE-SBP1

Evaluating Binding and Selectivity of SBP1 and TLHE-SBP1 to TTR

As can be seen in Figures 29 and 30, TLHE-SBP1 is able to selectively and potently bind

TTR in a reversible fashion. These data suggest that TLHE-SBP1 could demonstrate an

extension in the in vivo circulation half-life when compared to SBP1 alone.

Figure 29

Bar graph representation of percent occupancy of TTR in human serum by compounds in presence of FPE probe measured after 3 hours of incubation relative to probe alone
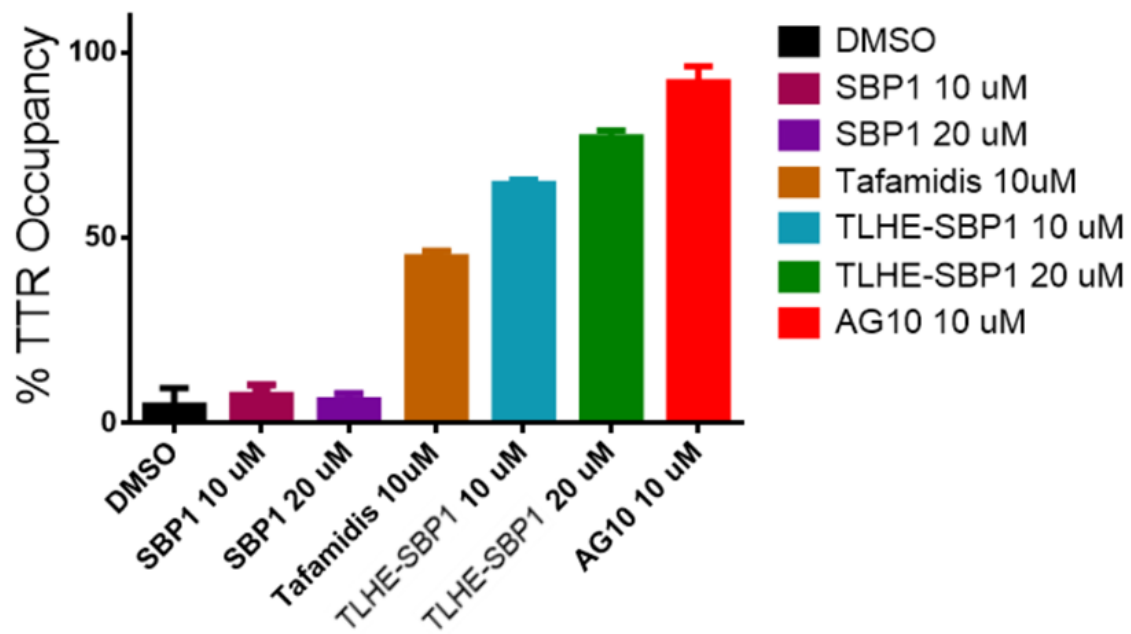
Figure 30

Binding affinity of TLHE-SBP1 and SBP1 to TTR in human serum. Fluorescence change caused by modification of TTR in human serum (TTR concentration, ~5 μM) by covalent FPE probe monitored for 6 hours in the presence of FPE probe alone (black circles) or probe and TTR ligands (colors; 10 μM or 20 μM). The lower the binding and fluorescence of the FPE probe, the higher is the binding and selectivity of ligand to TTR
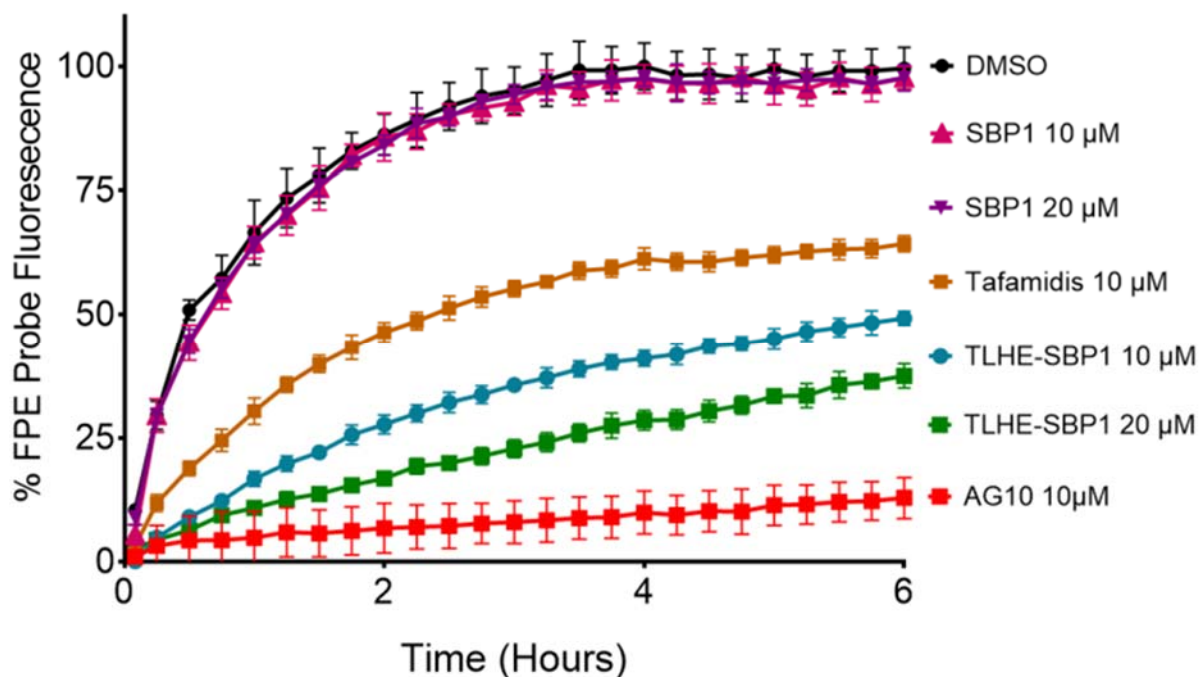
SARS-Cov-2-RBD via BLI

As depicted in Figures 31 and 32, the binding affinity of ACE2-Fc, SBP1, and TLHE-SBP1, was measured. A positive control of ACE2-Fc was utilized to validate the experiment and also to serve as a reference to compare SBP1 and TLHE-SBP1 binding to an immobilized fragment of the SARS-Cov-2 spike protein. TLHE-SBP1 was able to demonstrate comparable binding affinities to both the original SBP1 and the ACE2-Fc groups. This would indicate that conjugation of TLHE to the N-terminus of SBP1 did not interfere with binding.

Figure 31

Summary of results from BLI characterization of ACE2-Fc, SBP1, and TLHE-SBP1

Summary of BLI Results	
Ligand	Kd
ACE2-Fc	3.12E-08
SBP1	3.84E-08
TLHE-SBP1	3.22E-08

Figure 32

Results from BLI characterization of ACE2-Fc, SBP1, and TLHE-SBP1
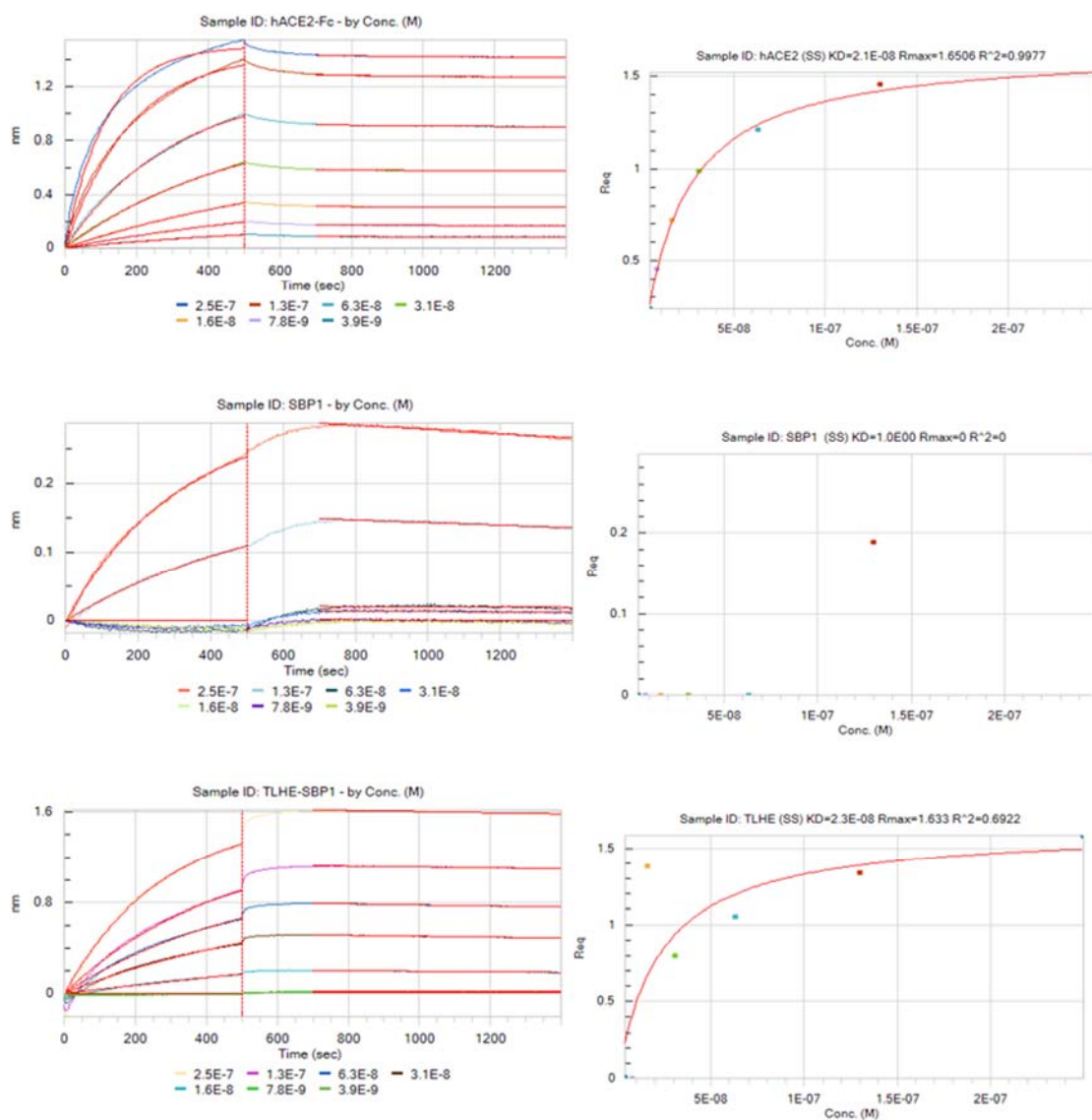
Pharmacokinetic Evaluation of SBP1 and TLHE-SBP1 in Male Sprague Dawley Rats

A summary of a pharmacokinetic evaluation in rats can be found in Figures 33 and 34 where a significant extension of circulation half-life can be observed.

Figure 33

Result of a pharmacokinetic study in Sprague Dawley rats measured through LC-MS
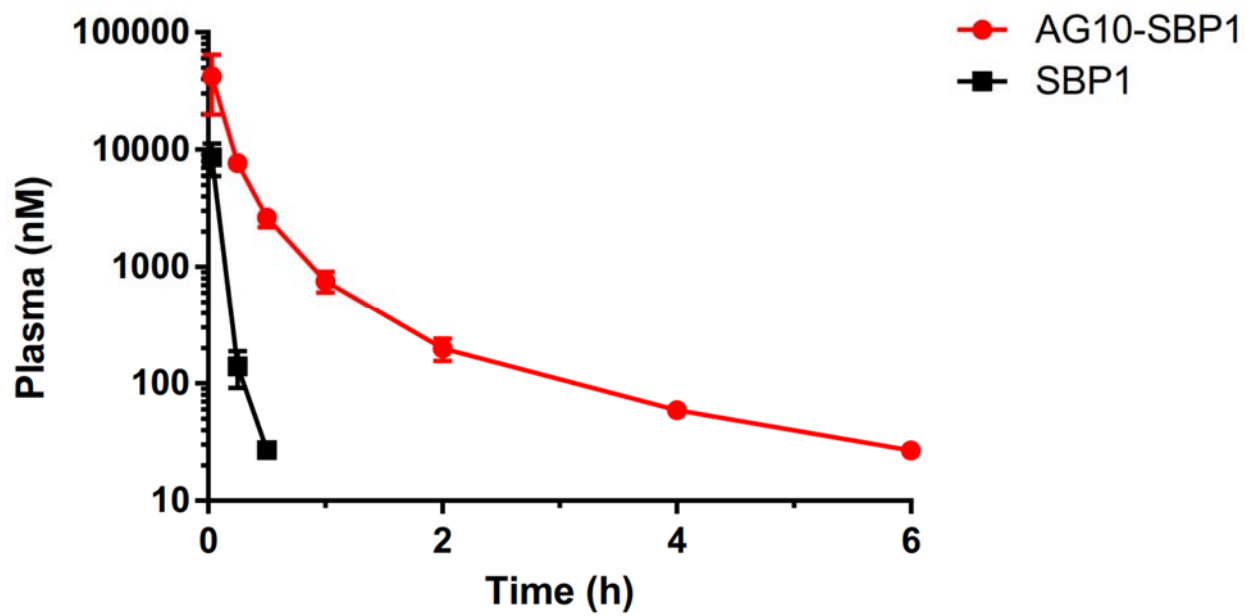
Figure 34

Calibration curves of SBP1 and TLHE-SBP1 for LC-MS/MS

SBP1 calibration1

$y = 0.0003x - 0.0121$
$R^2 = 0.9945$

TLHE-SBP1 calibration 1

$y = 0.0002x + 0.0423$
$R^2 = 0.9994$
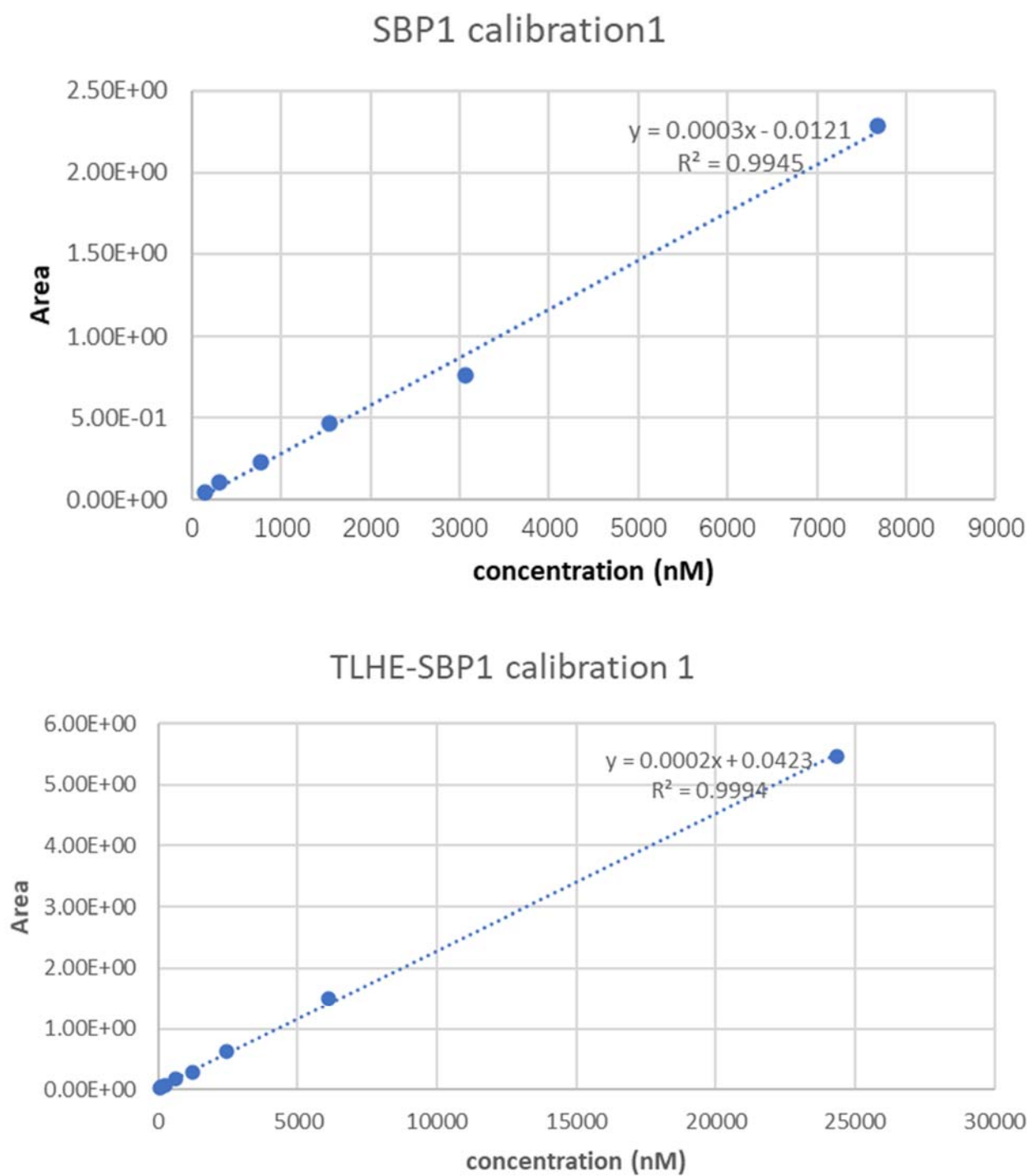
Live Reporter Virus Assay

In this assay, SBP1 and TLHE-SBP1 was unable to reduce the infectivity rate of live

SARS-Cov-2 viruses towards the host cell line. As can be seen in Figure 35, the ability of both

SBP1 and TLHE-SBP1 in viral entry inhibition was minimal at even micromolar concentrations.

Figure 35

Live virus reporter assay result from Dr. Jin Jing at Vitalant Research Institute
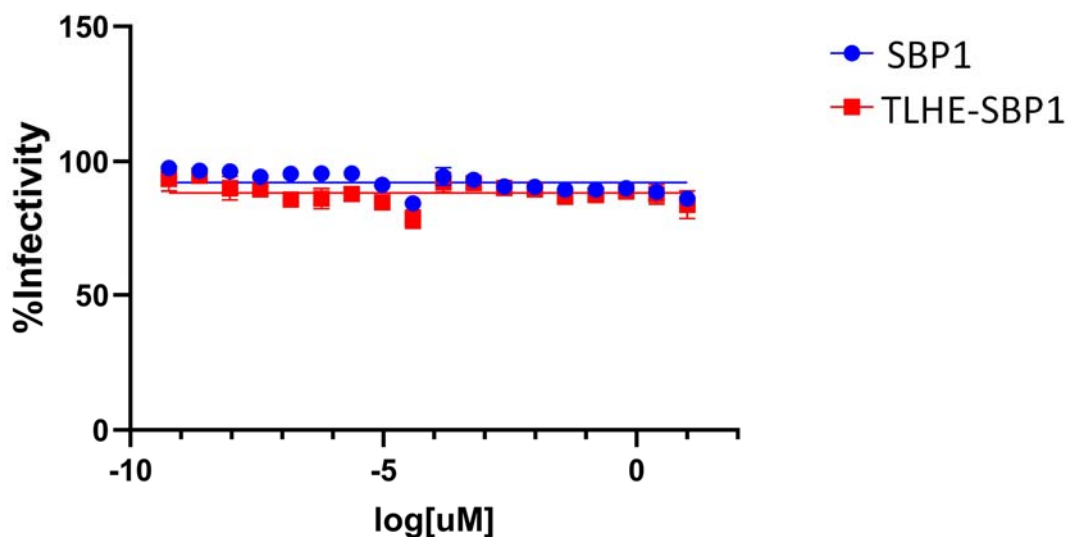
Discussion

Entry inhibitors are a unique approach to prevent viral infection propagation. Based on

the inspiration derived from famously successful drugs such as Enfuvirtide, we attempted to use

a publicly reported peptide sequence which mimicked the human ACE2 binding domain. This

mimic was intended to act as a decoy by interacting with the receptor binding domain of the

notorious spike protein integral to SARS-CoV-2 entry into pulmonary cells. The main limitation

in the utilization of SBP1 directly in the clinic was a very short circulation half-life which can be

seen in Figure 33. To this end, conjugation of SBP1 to TLHE successfully converted SBP1into a

viable option with enhanced half-life. More importantly, TLHE conjugation was able to confer

all the benefits of reversible TTR without compromising binding affinity. Unfortunately, both

SBP1 and TLH2-SBP1 did not show activity in live virus assay. It could be postulated that the

small size of both SBP1 and TLHE-SBP1 was the reason behind a lack of live virus entry

inhibition observed in Figure 35. Herein lies a major conundrum with our approach. The small

size of TLHE affords maintenance of binding affinity of SBP1, however that same small size

appears to be insufficient in providing the steric blockage necessary to prevent viral binding and

internalization. It is possible that a tri-plex style conglomerate of inhibitor peptide (SBP1 or

TLHE-SBP1), SARS-CoV-2, and the ACE2 receptor could still form. This would be one

explanation behind the poor viral entry inhibition despite comparable binding affinity data to

ACE2-Fc. Another argument could be that the ACE2-Fc fragment did not properly mimic the

true human ACE2 receptor, and therefore the virus interacted with the real receptor in a different

manner which the peptide decoy was not able to block.

References

1. Leader, B.; Baca, Q. J.; Golan, D. E. Protein Therapeutics: A Summary and Pharmacological Classification. *Nature Reviews Drug Discovery* 2008, *7* (1), 21–39. https://doi.org/10.1038/nrd2399.

2. Usmani, S. S.; Bedi, G.; Samuel, J. S.; Singh, S.; Kalra, S.; Kumar, P.; Ahuja, A. A.; Sharma, M.; Gautam, A.; Raghava, G. P. S. THPdb: Database of FDA-Approved Peptide and Protein Therapeutics. *PLOS ONE* 2017, *12* (7), e0181748. https://doi.org/10.1371/journal.pone.0181748.

3. Zaman, R.; Islam, R. A.; Ibnat, N.; Othman, I.; Zaini, A.; Lee, C. Y.; Chowdhury, E. H. Current Strategies in Extending Half-Lives of Therapeutic Proteins. *Journal of Controlled Release* 2019, *301*, 176–189. https://doi.org/10.1016/j.jconrel.2019.02.016.

4. Dutcher, J. P.; Schwartzentruber, D. J.; Kaufman, H. L.; Agarwala, S. S.; Tarhini, A. A.; Lowder, J. N.; Atkins, M. B. High Dose Interleukin-2 (Aldesleukin) - Expert Consensus on Best Management Practices-2014. *Journal for ImmunoTherapy of Cancer* 2014, *2* (1). https://doi.org/10.1186/s40425-014-0026-0.

5. Fletcher, A. M.; Tellier, P.; Douville, J.; Mansell, P.; Graziano, M. J.; Mangipudy, R. S.; Brodie, T. A.; Achanzar, W. E. Adverse Vacuolation in Multiple Tissues in Cynomolgus Monkeys Following Repeat-Dose Administration of a PEGylated Protein. *Toxicology Letters* 2019, *317*, 120–129. https://doi.org/10.1016/j.toxlet.2019.09.023.

6. Ju, Y.; Carreño, J. M.; Simon, V.; Dawson, K.; Krammer, F.; Kent, S. J. Impact of Anti-PEG Antibodies Induced by SARS-CoV-2 mRNA Vaccines. *Nature Reviews Immunology* 2022, *23* (3), 135–136. https://doi.org/10.1038/s41577-022-00825-x.

7. Fang, J.-L.; Beland, F. A.; Tang, Y.; Roffler, S. R. Flow Cytometry Analysis of Anti-Polyethylene Glycol Antibodies in Human Plasma. *Toxicology Reports* 2021, *8*, 148–154. https://doi.org/10.1016/j.toxrep.2020.12.022.

8. Zaghmi, A.; Mendez-Villuendas, E.; Greschner, A. A.; Liu, J. Y.; de Haan, H. W.; Gauthier, M. A. Mechanisms of Activity Loss for a Multi-PEGylated Protein by Experiment and Simulation. *Materials Today Chemistry* **2019**, *12*, 121–131. https://doi.org/10.1016/j.mtchem.2018.12.007.

9. Lear, S.; Amso, Z.; Shen, W. Engineering PEG-Fatty Acid Stapled, Long-Acting Peptide Agonists for G Protein-Coupled Receptors. *Methods in Enzymology* **2019**, 183–200. https://doi.org/10.1016/bs.mie.2019.02.008.

10. Rath, T.; Baker, K.; Dumont, J. A.; Peters, R. T.; Jiang, H.; Qiao, S.-W.; Lencer, W. I.; Pierce, G. F.; Blumberg, R. S. Fc-Fusion Proteins and FcRn: Structural Insights for Longer-Lasting and More Effective Therapeutics. *Critical Reviews in Biotechnology* **2013**, *35* (2), 235–254. https://doi.org/10.3109/07388551.2013.834293.

11. Liz, M. A.; Coelho, T.; Bellotti, V.; Fernandez-Arias, M. I.; Mallaina, P.; Obici, L. A Narrative Review of the Role of Transthyretin in Health and Disease. *Neurology and Therapy* **2020**, *9* (2), 395–402. https://doi.org/10.1007/s40120-020-00217-0.

12. Sanguinetti, C.; Minniti, M.; Susini, V.; Caponi, L.; Panichella, G.; Castiglione, V.; Aimo, A.; Emdin, M.; Vergaro, G.; Franzini, M. The Journey of Human Transthyretin: Synthesis, Structure Stability, and Catabolism. *Biomedicines* **2022**, *10* (8), 1906. https://doi.org/10.3390/biomedicines10081906.

13. Gonzalez-Duarte, A.; Ulloa-Aguirre, A. A Brief Journey through Protein Misfolding in Transthyretin Amyloidosis (ATTR Amyloidosis). *International Journal of Molecular Sciences* **2021**, *22* (23), 13158. https://doi.org/10.3390/ijms222313158.

14. Johnson, S. M.; Connelly, S.; Fearns, C.; Powers, E. T.; Kelly, J. W. The Transthyretin Amyloidoses: From Delineating the Molecular Mechanism of Aggregation Linked to Pathology to a Regulatory-Agency-Approved Drug. *Journal of Molecular Biology* **2012**, *421* (2–3), 185–203. https://doi.org/10.1016/j.jmb.2011.12.060.

15. Pinheiro, F.; Pallarès, I.; Peccati, F.; Sánchez-Morales, A.; Varejão, N.; Bezerra, F.; Ortega-Alarcon, D.; Gonzalez, D.; Osorio, M.; Navarro, S.; Velázquez-Campoy, A.; Almeida, M. R.; Reverter, D.; Busqué, F.; Alibés, R.; Sodupe, M.; Ventura, S. Development of a Highly Potent Transthyretin Amyloidogenesis Inhibitor: Design, Synthesis, and Evaluation. *Journal of Medicinal Chemistry* **2022**, *65* (21), 14673–14691. https://doi.org/10.1021/acs.jmedchem.2c01195.

16. Guo, X.; Liu, Z.; Zheng, Y.; Li, Y.; Li, L.; Liu, H.; Chen, Z.; Wu, L. <p>Review on the Structures and Activities of Transthyretin Amyloidogenesis Inhibitors</P>. *Drug Design, Development and Therapy* **2020**, *Volume 14*, 1057–1081. https://doi.org/10.2147/dddt.s237252.

17. Miller, M.; Pal, A.; Albusairi, W.; Joo, H.; Pappas, B.; Haque Tuhin, M. T.; Liang, D.; Jampala, R.; Liu, F.; Khan, J.; Faaij, M.; Park, M.; Chan, W.; Graef, I.; Zamboni, R.; Kumar, N.; Fox, J.; Sinha, U.; Alhamadsheh, M. Enthalpy-Driven Stabilization of Transthyretin by AG10 Mimics a Naturally Occurring Genetic Variant That Protects from Transthyretin Amyloidosis. *Journal of Medicinal Chemistry* **2018**, *61* (17), 7862–7876. https://doi.org/10.1021/acs.jmedchem.8b00817.

18. Cioffi, C. L.; Raja, A.; Muthuraman, P.; Jayaraman, A.; Jayakumar, S.; Varadi, A.; Racz, B.; Petrukhin, K. Identification of Transthyretin Tetramer Kinetic Stabilizers That Are Capable of Inhibiting the Retinol-Dependent Retinol Binding Protein 4-Transthyretin Interaction: Potential Novel Therapeutics for Macular Degeneration, Transthyretin Amyloidosis, and Their Common Age-Related Comorbidities. *Journal of Medicinal Chemistry* **2021**, *64* (13), 9010–9041. https://doi.org/10.1021/acs.jmedchem.1c00099.

19. Spolski, R.; Li, P.; Leonard, W. J. Biology and Regulation of IL-2: From Molecular Mechanisms to Human Therapy. *Nature Reviews Immunology* **2018**, *18* (10), 648–659. https://doi.org/10.1038/s41577-018-0046-y.

20. Dutcher, J. P.; Schwartzentruber, D. J.; Kaufman, H. L.; Agarwala, S. S.; Tarhini, A. A.; Lowder, J. N.; Atkins, M. B. High Dose Interleukin-2 (Aldesleukin) - Expert Consensus on Best Management Practices-2014. *Journal for ImmunoTherapy of Cancer* **2014**, *2* (1). https://doi.org/10.1186/s40425-014-0026-0.

21. Whole Gel Eluter and Mini Whole Gel Eluter https://www.bio-rad.com/en-us/product/whole-gel-eluter-mini-whole-gel-eluter?ID=3d6b2ca7-5472-4251-ae7b-bbaf71be3a0c. (BioRad Mini Whole Gel Eluter Product Manual)

22. https://www.bio-rad.com/sites/default/files/webroot/web/pdf/lsr/literature/M1652976B.pdf (Model 422 Electro Eluter Product Manual)

23. Murakami, N.; Hayden, R.; Hills, T.; Al-Samkari, H.; Casey, J.; Del Sorbo, L.; Lawler, P. R.; Sise, M. E.; Leaf, D. E. Therapeutic Advances in COVID-19. *Nature Reviews Nephrology* **2022**, *19* (1), 38–52. https://doi.org/10.1038/s41581-022-00642-4.

24. Chitsike, L.; Duerksen-Hughes, P. Keep out! SARS-CoV-2 Entry Inhibitors: Their Role and Utility as COVID-19 Therapeutics. *Virology Journal* **2021**, *18* (1). https://doi.org/10.1186/s12985-021-01624-x.

25. Morgan, D. A.; Ruscetti, F. W.; Gallo, R. Selective in Vitro Growth of T Lymphocytes from Normal Human Bone Marrows. *Science* **1976**, *193* (4257), 1007–1008. https://doi.org/10.1126/science.181845.

26. Castro, I.; Yu, A.; Dee, M. J.; Malek, T. R. The Basis of Distinctive IL-2– and IL-15– Dependent Signaling: Weak CD122-Dependent Signaling Favors CD8+ T Central-Memory Cell Survival but Not T Effector-Memory Cell Development. *The Journal of Immunology* **2011**, *187* (10), 5170–5182. https://doi.org/10.4049/jimmunol.1003961.

27. Rickert, M., Wang, X., Boulanger, M. J., Goriatcheva, N. & Garcia, K. C. Structural Biology: The structure of interleukin-2 complexed with its alpha receptor. *Science (80-.).* 308, (2005).

28. Wang, X., Rickert, M. & Garcia, K. C. Structure of the Quaternary Complex of Interleukin-2 with Its α, ß, and γ<sub>c</sub> Receptors. *Science (80-.).* 310, (2005).

29. Rickert, M., Boulanger, M. J., Goriatcheva, N. & Garcia, K. C. Compensatory energetic mechanisms mediating the assembly of signaling complexes between interleukin-2 and its α, β, and γc receptors. *J. Mol. Biol.* 339, (2004).

30. Liang, S. M.; Allet, B.; Rose, K.; Hirschi, M.; Liang, C. M.; Thatcher, D. R. Characterization of Human Interleukin 2 Derived from Escherichia Coli. *Biochemical Journal* 1985, *229* (2), 429–439. https://doi.org/10.1042/bj2290429.

31. Bhatwa, A.; Wang, W.; Hassan, Y. I.; Abraham, N.; Li, X.-Z.; Zhou, T. Challenges Associated With the Formation of Recombinant Protein Inclusion Bodies in Escherichia Coli and Strategies to Address Them for Industrial Applications. *Frontiers in Bioengineering and Biotechnology* 2021, *9*. https://doi.org/10.3389/fbioe.2021.630551.

32. Wang, Y.; van Oosterwijk, N.; Ali, A. M.; Adawy, A.; Anindya, A. L.; Dömling, A. S. S.; Groves, M. R. A Systematic Protein Refolding Screen Method Using the DGR Approach Reveals That Time and Secondary TSA Are Essential Variables. *Scientific Reports* 2017, *7* (1). https://doi.org/10.1038/s41598-017-09687-z.

33. Arkin, M. R.; Randal, M.; DeLano, W. L.; Hyde, J.; Luong, T. N.; Oslob, J. D.; Raphael, D. R.; Taylor, L.; Wang, J.; McDowell, R. S.; Wells, J. A.; Braisted, A. C. Binding of Small Molecules to an Adaptive Protein–Protein Interface. *Proceedings of the National Academy of Sciences* 2003, *100* (4), 1603–1608. https://doi.org/10.1073/pnas.252756299.

34. Goodson, R. J.; Katre, N. V. Site-Directed Pegylation of Recombinant Interleukin-2 at Its Glycosylation Site. *Nature Biotechnology* 1990, *8* (4), 343–346. https://doi.org/10.1038/nbt0490-343.

35. Weir, M. P.; Sparks, J. Purification and Renaturation of Recombinant Human Interleukin-2. *Biochemical Journal* 1987, *245* (1), 85–91. https://doi.org/10.1042/bj2450085.

36. Kato, K.; Yamada, T.; Kawahara, K.; Onda, H.; Asano, T.; Sugino, H.; Kakinuma, A. Purification and Characterization of Recombinant Human Interleukin-2 Produced in Escherichia Coli. *Biochemical and Biophysical Research Communications* 1985, *130* (2), 692–699. https://doi.org/10.1016/0006-291x(85)90472-3.

37. Abuchowski, A.; van Es, T.; Palczuk, N. C.; Davis, F. F. Alteration of Immunological Properties of Bovine Serum Albumin by Covalent Attachment of Polyethylene Glycol. *Journal of Biological Chemistry* 1977, *252* (11), 3578–3581. https://doi.org/10.1016/s0021-9258(17)40291-2.

38. SAMINENI, R.; CHIMAKURTHY, J.; KONIDALA, S. Emerging Role of Biopharmaceutical Classification and Biopharmaceutical Drug Disposition System in Dosage Form Development: A Systematic Review. *Turkish Journal of Pharmaceutical Sciences* 2022, *19* (6), 706–713. https://doi.org/10.4274/tjps.galenos.2021.73554.

39. Tomar, D.; Khan, T.; Singh, R. R.; Mishra, S.; Gupta, S.; Surolia, A.; Salunke, D. M. Crystallographic Study of Novel Transthyretin Ligands Exhibiting Negative-Cooperativity between Two Thyroxine Binding Sites. *PLoS ONE* 2012, *7* (9), e43522. https://doi.org/10.1371/journal.pone.0043522.

40. Liz, M. A.; Gomes, C. M.; Saraiva, M. J.; Sousa, M. M. ApoA-I Cleaved by Transthyretin Has Reduced Ability to Promote Cholesterol Efflux and Increased Amyloidogenicity. *Journal of Lipid Research* 2007, *48* (11), 2385–2395. https://doi.org/10.1194/jlr.m700158-jlr200.

41. Zhang, G.; Pomplun, S.; Loftis, A. R.; Tan, X.; Loas, A.; Pentelute, B. L. Investigation of ACE2 N-Terminal Fragments Binding to SARS-CoV-2 Spike RBD. **2020**. https://doi.org/10.1101/2020.03.19.999318.

42. Moore, J. P.; Doms, R. W. The Entry of Entry Inhibitors: A Fusion of Science and Medicine. *Proceedings of the National Academy of Sciences* **2003**, *100* (19), 10598–10602. https://doi.org/10.1073/pnas.1932511100.